SPP7 Conference

Poster Presentations

Part I

June 4, 2015

SERS Spectroscopy of Living Cells with Three-Dimensional Plasmonic Nanoantennas

Rosanna La Rocca, Gabriele C. Messina, Michele Dipalo, Victoria Shalabaeva,
Francesco De Angelis
Nanostructures, Fondazione Istituto Italiano di Tecnologia, Genova, Italy

Presently, fluorescence microscopy represents the standard technique for living cells analysis. However, it still presents critical disadvantages such as bleaching or the necessity of labels, which limit the amount of observable features. A promising alternative could be Raman spectroscopy, which, differently from fluorescence, has the potential to give a complete picture of the cell chemical environment without using target labels. The present main limitation of Raman spectroscopy is its extremely low sensitivity that leads to unsuitable detection limits in biology. In order to increase Raman sensitivity, we propose to use three-dimensional (3D) plasmonic nanoantennas directly fabricated on cell culture substrates. It has already been proven that 3D plasmonic nanoantennas present significantly high plasmonic field enhancement[1] when coated with silver. Nevertheless, silver is a cytotoxic material; therefore, here we evaluates the performance of gold-silver 3D nanoantennas for SERS analysis of living cells.

Arrays of nanoantennas placed with various arrangements were fabricated on silicon nitride membranes. A silver/gold bilayer (30 + 7 nm) was deposited homogenously on the membrane/nanoantennas system. Neuro 2A and fibroblast 3T3 cell lines were cultured on these substrates to study biocompatibility. Results were observed by electron and confocal microscopy. Both cell lines adhered and proliferated on the membranes.

Raman spectroscopy was performed directly on living cells in their cell media. A near-IR source (785 nm) was used for reducing light absorption and cell photo-damage. Raman spectra acquired at low light intensities on nanoantennas showed distinctive peaks of relevant biomolecules, whereas spectra acquired on the gold surface with the same acquisition parameters did not show any significant peak. These results show that 3D nanoantennas are extremely promising tools for the analysis of living cells.

References:

De Angelis, F. *et al.*3D hollow nanostructures as building blocks for multifunctional plasmonics. *Nano Lett.* **13,** 3553–8 (2013).

Acknowledgment

The research has received funding from the European Research Council under the European Union`s Seventh Framework Programme (FP/2007-2013) / ERC Grant Agreement n. [616213], CoG: Neuro-Plasmonics.

francesco.deangelis@iit.it

Wafer-Scale Photonic and Plasmonic Crystal Sensors

Matthew C. George[1], Jui-Nung Liu[2], Arash Farhang[1], Brent Williamson[1], Mike Black[1], Ted Wangensteen[1], James Fraser[1], Rumyana Petrova[1], Brian T. Cunningham[2]

[1]*Optics Department, Moxtek, Inc., Orem, USA*

[2]*Electrical and Computer Engineering, University of Illinois at Urbana-Champaign, Urbana, USA*

200 mm diameter wafer-scale fabrication, metrology, and optical modeling results will be reviewed for surface plasmon resonance (SPR) sensors based on 2D metallic nano-dome and nano-hole arrays (NHA) as well as 1D photonic crystal sensors based on leaky-waveguide mode resonance, with potential applications in label free sensing, surface enhanced Raman spectroscopy (SERS), and surface-enhanced fluorescence spectroscopy (SEFS). Potential markets include micro-arrays for medical diagnostics, forensic testing, environmental monitoring, and food safety.

Wafer-scale optical metrology results will be compared to FDTD modeling and presented along with application-based performance results, including label-free plasmonic and photonic crystal sensing of both surface binding kinetics and bulk refractive index changes. In addition, SERS and SEFS results from a line scan microscope system will be presented for several 1D photonic crystal and 2D metallic array structures. Figure 1 presents fabrication and optical metrology results for various 1D and 2D photonic crystal and SPR sensors. Narrow-band photonic crystal resonance sensors showed quality factors over 200, although wafer-uniformity needs further improvement. Gold-coated nano-dome arrays for SERS applications showed gaps with spacing in the 10-20 nm range. Normal incidence extraordinary optical transmission (EOT) results for a 550 nm pitch nano-hole array showed good bulk refractive index sensitivity, however an intensity-based design with 665 nm pitch was chosen for use as a compact, label-free sensor at both 650 and 632.8 nm wavelengths. The optimized NHA sensor gives an SPR shift of about 480 nm per refractive index unit when detecting a series of 0-40% glucose solutions.

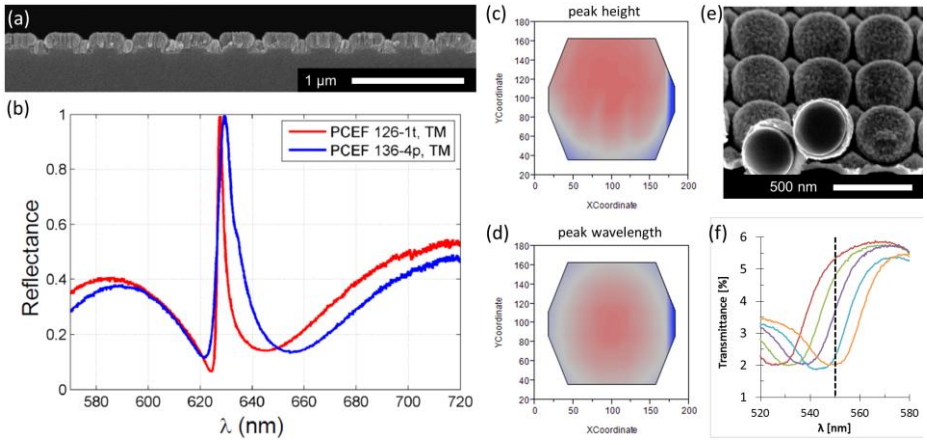

Figure 1. (a)-(d) Results for narrow band 1D photonic crystal sensors composed of TiO_2 layer on SiO_2 grating. (a) SEM cross-section, (b) normal incidence Reflectance, and 200mm diameter wafer maps for 7.5° reflectance showing (c) peak height and (d) peak wavelength uniformity. Red color corresponds to larger Reflectance or longer λ. (e) Au-coated nano-dome array sample. (f) EOT at normal incidence for 550 nm pitch NHA under 0-40% aqueous glucose solutions.

mgeorge@moxtek.com

A Fast Assay to Determine Infliximab Trough Level using Fiber-Optic Surface Plasmon Resonance Sensor

Jiadi Lu[1], Thomas Van Stappen[2], Dragana Spasic[1], Filip Delport[1], Ann Gils[2], Jeroen Lammertyn[1]

[1]*Department of Biosystems, MeBioS, Leuven, Belgium*

[2]*Department of Pharmaceutical and Pharmacological Sciences, Laboratory for Therapeutic and Diagnostic Antibodies, Leuven, Belgium*

Therapeutic monoclonal antibodies, such as Infliximab (IFX) are highly effective for treating inflammatory bowel disease patients. It is recommended to monitor the trough level of IFX for improving therapeutic outcome of the bimonthly treatment [1]. The conventionally used ELISA assay is time-consuming and not optimal for single patient testing. Here, we present a fiber-optic surface plasmon resonance (FO-SPR) sensor [2] as a potential point-of-care diagnostic tool (Figure 1). On this platform, surface plasmon waves are generated at the interface of an optical fiber/gold layer (50 nm). On top of this gold layer through a self-assembly monolayer (SAM), an in-house developed IFX-specific monoclonal antibody is immobilized to establish a sandwich immunoassay. Analysis was performed on IFX spiked serum in 100 fold diluted serum obtained from healthy volunteers. The signal was specifically amplified by a second IFX-specific detection antibody conjugated to 20 nm gold nanoparticles. An IFX calibration curve was made, ranging from 0 to 75 ng/ml, using a single fiber with surface regeneration in between measurements. The limit of detection from 6 calibration curves (Figure 2) was 2.17 ng/ml, corresponding to 0.22 µg/ml in the whole serum. This bio-assay was further validated with 5 patient samples and corresponding IFX concentrations were determined based on the FO-SPR calibration curves. This work demonstrates the potential of the FO-SPR platform to be used at the point-of-care for improving the therapeutic outcome of patients treated with IFX.

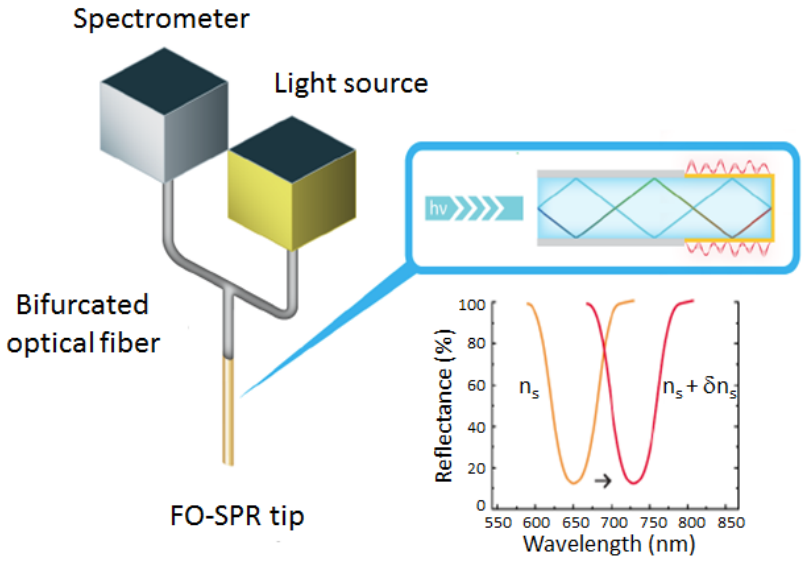

Figure 1. Concept scheme of the FO-SPR sensor. It can be seen that SPRs are excited by incident photons at the interface of fiber/gold layer, where any change in refractive index due to interactions between biomolecules will be indicated by the wavelength shift.

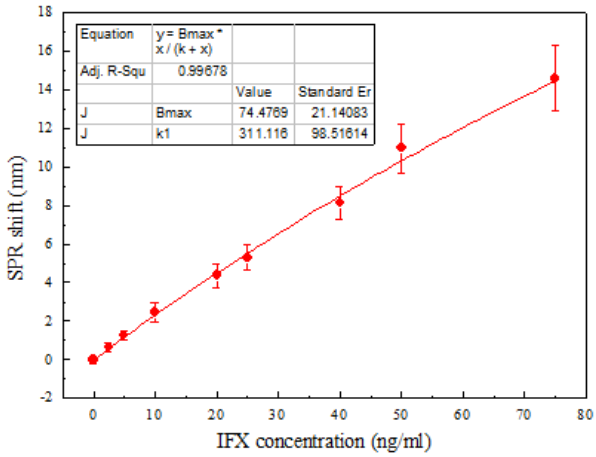

Figure 2. Calibration curve with series of IFX diluted in serum (100 fold dilution) ranging from 0 to 75 ng/ml. Error bars represent standard deviation (n = 6).

[1] S. Vermeire, A. Gils. Frontline Gastroenterol. Jan 2013; 4(1): 41–43

[2] J. Pollet et al., Talanta 2011; 83: 1436-1441

Jiadi.Lu@biw.kuleuven.be

Ultrasensitive Label-Free Biosensor Based on Photon Crystal Surface Waves: a Tool to Study Dynamics of Receptor-Ligand Interactions with Living Bacteria and Cells

Serguei Sekatskii, Ekaterina Rostova, Giovanni Dietler
Laboratoire de Physique de la Matiére Vivante, Ecole Polytechnique Fédérale de Lausanne (EPFL), Lausanne, Switzerland

Recently, we presented a label-free biosensor based on registration of photonic crystal surface waves and discussed its first applications to study not only such "standard" systems as rabbit and mouse IgG and anti-rabbit and anti-mouse IgG protein pairs [1] but also earlier unexplored kinetics of Laminin Binding Protein (LBP) – flaviviral surface protein *E* interaction, which enabled (in combination with Single Molecule Dynamic Force Spectroscopy studies) unambiguously demonstrate force induced globule-coil transition of LBP and its complexes; the process which is of an uttermost importance for the viral – cell membrane fusion [2]. Angular interrogation of the optical surface wave resonance is used to detect changes in the thickness of an adsorbed layer, while an additional detection of the critical angle of total internal refection provides independent data on the liquid refraction index, see Fig. 1. Besides segregation of surface and volume effects, the exploitation of Photonic Crystal supporting long propagated surface waves enables to achieve mass sensitivity at the level of 0.3 pg/mm^2 and refraction index (RI) sensitivity at the level of 10^{-7} RIU/Hz$^{1/2}$.

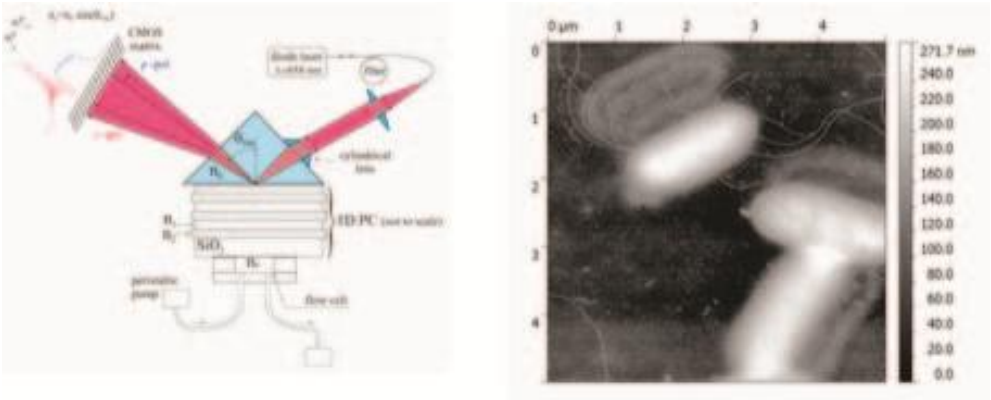

Figure 1. Left: Schematic of the biosensor. Right: AFM image of (mono)layer of *E. coli* bacteria used as a generic "immobilized receptor layer" in the sensor.

Other characteristic feature of this biosensor is large, of the order of 1 micron, surface wave penetration depth into an external media, which enables to study intermolecular interactions not only at (a few) monolayers level, but also for such large objects as viruses, bacteria and cell organells. Here we report the first steps in this direction. We elaborated a chitosan-based protocol of surface modification of the sensor chip enabling to produce sufficiently dense and homogeneous (mono)layers of live *E. coli* bacteria (see Fig. above), and then these layers have been exploited as a generic "immobilized receptor layer" to study kinetics of adsorption of different ligands onto their (i.e. bacteria's) surface.

Konopsky, V. N. *et al*., *Sensors,* **2013,** *13*, 2566.

Zaitsev, B. N. *et al*., *J. Molecular Recognition,* **2014,** *27*, 727.

serguei.sekatski@epfl.ch

Blue and UV Surface Plasmonics and Sensor Application

Dmitry Basmanov[1], **Serguei Sekatskii**[2], Elena Alieva[3], Valery Konopsky[3], Giovanni Dietler[2], Dmitry Klinov[1]

[1]*Department of Biophysics, Russian Institute for Physical-Chemical Medicine, Moscow, Russia*

[2]*Laboratoire de Physique de la Matière Vivante, Ecole Polytechnique Fédérale de Lausanne, Lausanne, Switzerland*

[3]*Solid State Spectroscopy Department, Institute of spectroscopy RAS, Moscow, Russia*

We demonstrate effective surface plasmon propagation along thin gold nanofilm in a blue and UV spectral ranges. We used specially designed one dimentional photonic crystal: silica substrate/H(LH)8/H'M/gas, where H is a Ta_2O_5 layer with the thickness 57.8 nm, L is a SiO_2 layer with the thickness 84.4 nm, H' is a Ta_2O_5 layer with the thickness of 55 nm and M is a 8 nm-thick gold layer. The scheme of the experimental setup is similar to the Kretschmann configuration. We used p-polarized 405 nm laser light to excite blue surface plasmons. The calculated dispersion diagram of the 1D photonic crystal structure used to support blue surface plasmon propagation (See Figure).

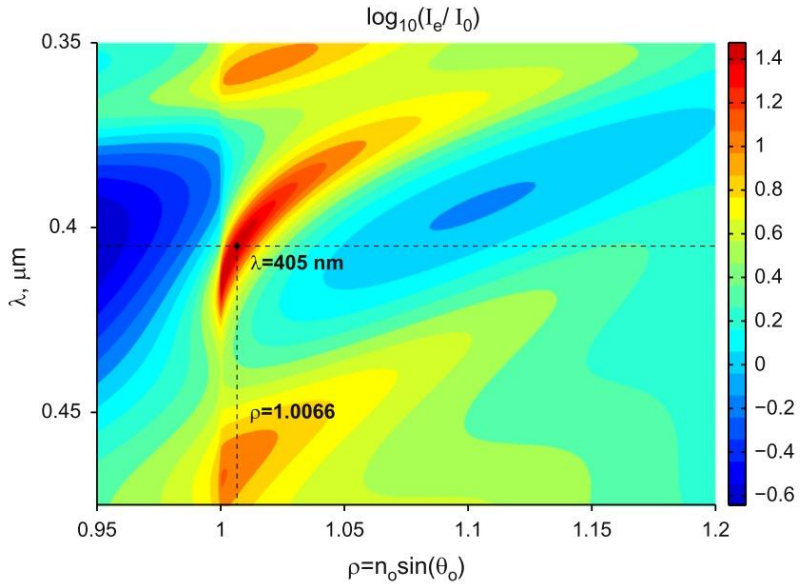

For 405 nm wavelength this structure supports ultralong surface plasmon propagation. An electromagnetic field intensity enhancement equals to 45. Calculated width of resonance dip for the presented structure is 0.4 degree, and the plasmon propagation distance equals to 10 um. For comparison, without the photonic crystal as small propagation length as 0.7 um is attained. Our experiments revealed that the structure at hand does support ultralong surface plasmon propagation, and the angular width of the plasmon excitation peak about 0.6 degree, thus corresponding to the plasmon propagation distance as long as 7 um.This structure and this technique have been tested as a sensor to detect small concentrations of nitrogen dioxide in air. The changes of the light intensity distribution onto the detector caused by the changes of the plasmon excitation conditions are measured. Based on the of our experiments, we estimate the attained limit of the reliable detection of nitrogen dioxide as ca. 3–4 ppm.

The results presented attest an experimental realization of effective surface plasmon propagation in blue and UV spectral ranges.

dmitry.basmanov@ripcm.org.ru

Synthesys of Metal-Dielectric Structure for Creating Optical Biosensors

Victor A. Simonov[1], Vadim Terentyev[1], Nina Goldina[2]
[1]*SB RAS, Institute of Automation and Electrometry, Novosibirsk, Russia*
[2]*SB RAS, Institute of Laser Physics, Novosibirsk, Russia*

Analysis of various metal-dielectric structures at angles of incidence greater than the critical angle is of the interest for biochemical environment sensors. Angular and spectral dependence of the reflection coefficient of the two structures - one with aluminum film and two-layer combination of the same film with a dielectric layer of zinc sulphide - are calculated and experimentally measured.

In reflected light at angles of incidence greater than the critical value, at the boundary of two dielectric media with a thin metal film between them, the frustrated total internal reflection appears at the resonant dependence of the reflection coefficient R with incident angle or wavelength. The appearance of the dips in the angular dependence of the reflectance of p-polarized light R_p is due to the excitation of surface plasmons [1]. Compact thin-layer sensor structures with a metal film are highly sensitive to refractive index changes in the analyzed liquids and gases [1-2].

The experimental scheme consists of a simple device - a prism with a thin metal film on the hypotenuse side, which is called a Kretchman configuration. It is interesting to analyze the R dependence transformation with various metal and dielectric layers combinations. Adding a dielectric layer enhances resonance effect. The first figure shows the calculated data for aluminum films with different thicknesses (7-18 nm). The optical constants for a massive aluminum ($n = 0.9 - i6.21$, $\lambda = 532$ nm), taken from the handbook, were used for modeling. It is clear, that minimum R_p shifts to lower angles with metal film thickness increasing. The second figure shows the experimental angular dependence of the pure aluminum film and the one with an added layer of ZnS. The figure shows that additional dielectric layer shifts the minimum R_p to smaller angles. Interesting results were obtained by measuring the spectral characteristics for the combination of Al + ZnS at different angles of incidence.

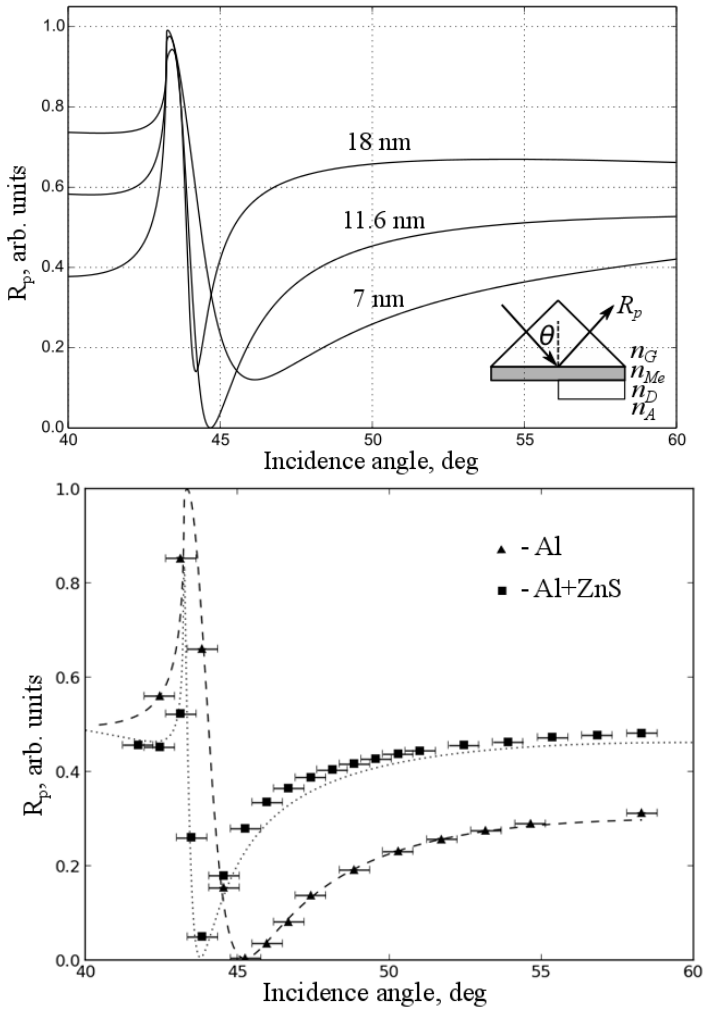

Our work is supported by the Russian Foundation for Basic Research (Grant No. 14-02-00248).

Shalabney A., Abdulhalim I. Figure-of-merit enhancement of surface plasmon resonance sensors in the spectral interrogation. Opt. Lett., 2012, **37** (7), 1175-1177.

Goldina N.D.. Frustrated total internal reflection from thin-layer structures with a metal film. Optics and Spectroscopy, 2009, Vol. 106, No. 5, pp. 748–752.

ngold@laser.nsc.ru

Extra-Ordinary Optical Transmission based Self-Referenced Sensor utilizing Nanosized Metallic Gratings

Sachin Kumar Srivastava[1], Mark Auslander[2], Ibrahim Abdulhalim[1,3]
[1]*Department of Electrooptic Engineering and Ilse Katz Institute for Nanoscale Science and Technology, Ben Gurion University of the Negev, Beer Sheva, Israel*
[2]*Department of Electrical and Computer Engineering, Ben-Gurion University of the Negev, Beer-Sheva, Israel*
[3]*School of Materials Science and Engineering, Nanyang Technological University, Singapore, Singapore*

We have simulated and fabricated a nanometallic grating of Au for the detection of small amounts of water in ethanol, which is very crucial for its use in medical field. The sensor works on the principle of extra-ordinary optical transmission (EOT) [1]. The nanograting was designed to work as a self referenced sensor in the optical telecommunications NIR window of the electromagnetic spectrum. The performance of the nanograting was optimized numerically with respect to substrate, material, cover layer, adhesion layer, metal film thickness, cover layer thickness, groove width, grating pitch, angle of incidence, and fabrication tolerance etc. before it fabricated. Figure 1(a) presents the recorded transmission spectra while 1(b) represents the response curve of the sensor. In figure 1(a), it is observed that two peaks are observed in the transmission spectrum for any analyte medium on the cover of the nanograting. Moreover, with an increase in the refractive index of the analyte medium, the resonance peak at the smaller wavelengths (first resonance) shows a red shift, while the one at the higher wavelength (second resonance) remains fixed at that wavelength. The first resonance peak is attributed to the plasmons at the analyte-grating interface while the second one to the plasmons at the grating-substrate interface as was confirmed by Karabchevsky et.al. [2]. In figure 1(b), we have plotted the variation of the first resonance peak with the change in the concentration of water in ethanol. This behaviour is exactly the same as reported previously by a SPR sensor [3]. The increase in the resonance wavelength until 20 percent water in ethanol is because of the formation of ethanol-water clusters due to formation of hydrogen bonds which become homogeneous after this concentration, leading to decrease in resonance wavelength [3]. Thus, this chip can work as a self-referenced sensor. The present nanograting is further in the process of utilization for blood analytes detection.

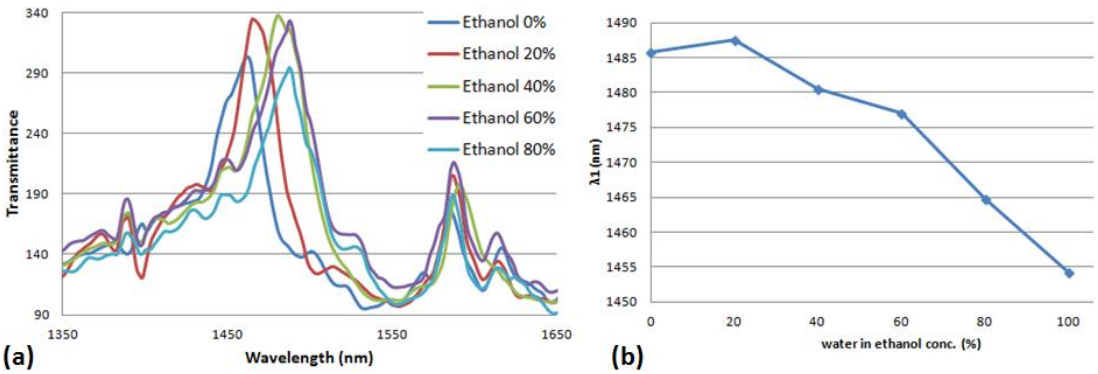

References

[1]. Ebbesen, et.al. Nature **391**, 667-669 (1998).

[2]. Karabchevsky et.al. J. Nanophoton. **5,** 051821 (2011).

[3]. Srivastava et.al. Sens. Act. B **153**, 194-198 (2011).

sachinchitransh@gmail.com

Polarimetric Spectral Surface Plasmon Resonance Sensor

Ibrahim Watad, Ibrahim Abdulhalim
Department of Electro-optic Engineering, Ben-Gurion University of the Negev, Beer-Sheeva, Israel

Intensity based surface plasmon resonance (SPR) sensors are widely used, but they still lack the sensitivity of detection, especially of low analyte concentrations. Profiting from the sharp jump in phase under SPR, we suggest working with this aspect in the spectral domain, which is more sensitive than the angular domain and its polarimetric properties were not investigated thoroughly. The prism and sample are between a polarizer and an analyzer and for each measurement of the phase difference we took three intensity measurements at three different orientations of the polarizer\analyzer. Measurements at different concentrations of Ethanol in Water were carried out using several polarimetric siganls and compared to the intensity measurements. The maximal value of the cosine of the phase shift between the p and s-polarization components of the reflected wave is found to be much better defined than the minimum value in the intensity. This leads to a better sensitivity and a lower detection limit.

References:

[1] Y. H. Huang, H. P. Ho, S. K. Kong, and A. V. Kabashin, Ann. Phys. (Berlin) 524, No. 11, 637-662 (2012).

[2] A. Shalabney and I. Abdulhalim, Laser Photonics Rev. 5, No. 4, 571-606 (2011).

watadib@post.bgu.ac.il

Exploring Plasmonic Resonances of Silver Capped Silicon Nanopillars

Kaiyu Wu, Michael Schmidt, Tomas Rindzevicius, Klaus Mogensen, Anja Boisen

Department of Micro- and Nanotechnology, Technical University of Denmark, Kgs. Lyngby, Denmark

Etching without applying a lithographic step can be used as a novel way of controllably fabricating large-area plasmonicnanopillar structures (NPs) in extremely short time [1]. However, the localized surface plasmonic resonance (LSPR) modes of NPs remain unknown. Here, we present LSPR properties of the NPsacquired by 3D FEM simulations and dark-field scattering measurements. The simulation results reveal that a silver capped silicon NP exhibits a strong LSPR resonance which couples through the Si cavity. This mode is distinguished by the enhanced localized fields near the neck of the silver cap, and its wavelength is found dominatedonly by the diameter of the Si pillar. Surprisingly, it is found that the resonance energy of such a cavity mode cannot be tuned via leaning of the pillars towards their nearest neighbors. The scattering measurements are in agreement with the simulation results and support the conclusions drawn from the simulations. The measured scattering peaks are broad, due to the slight variation inthe fabricated NPs geometries.The above mentioned results open for the possibility of developing the substrate towards a multifunctional plasmonic sensing platform that fulfills all the requirements of an ideal LSPR substrate for various sensing applications.

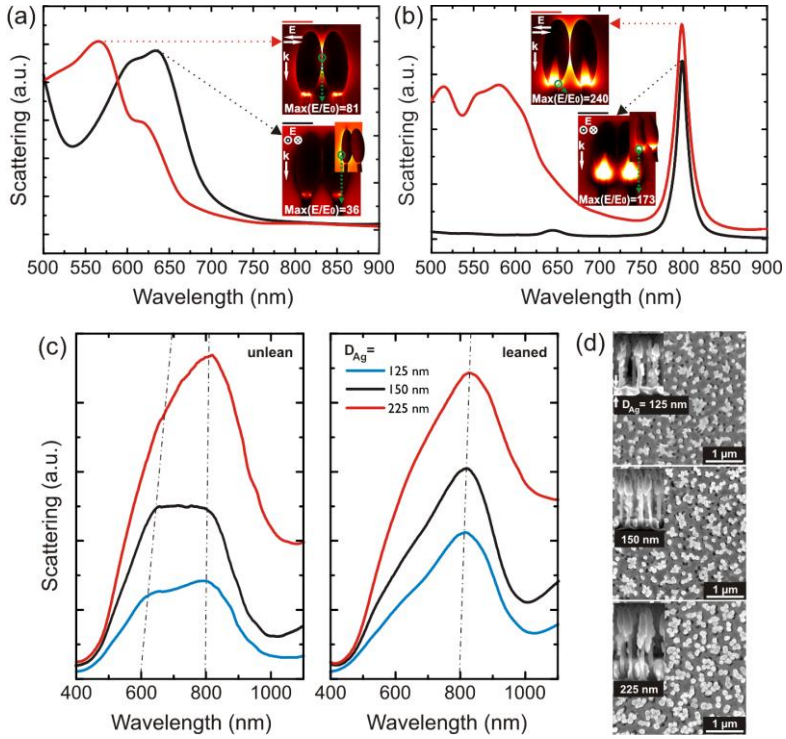

Figure 1. (a) Calculated scattering spectra for a dimer of Ag@Si NPs without Si cavities (the Si inside the Ag caps are replaced by Ag) under different polarization directions. (b) Same as (a), but for the case that the NPs contain Si cavities inside their Ag caps. (c) Measured scattering spectra for NPs on three substrates with different Ag deposition thicknesses: 125 nm, 150 nm, and 225 nm. (d) SEM images of leaning NPs (top view), Insets: cross-sectional view of the NPs before leaning.

[1] M. S. Schmidt, J. Hübner, A. Boisen, Advanced Materials, 24 (2012) 11-18.

kaiwu@nanotech.dtu.dk

A Low-Cost, High-Sensitivity Surface Enhanced Raman Scattering Substrate by Si Nanowire Arrays Decorated with Au Nanoparticles and Backplanes

Bi-Shen Lee[1], Ding-Zheng Lin[2], **Ta-Jen Yen**[1]
[1]*Department of Materials Science and Engineering, National Tsing Hua University, Hsinchu, Taiwan*
[2]*Department of Material and Chemical Research Laboratories, Industrial Technology and Research Institute (ITRI), Hsinchu, Taiwan*

Raman spectra provide rich vibrational signals that represent the fingerprint of molecules, and more importantly, such signals are insensitive to water so that recently the technique of Raman scattering emerges a promising method for environmental and biological trace analysis. Nevertheless, the scattering cross section of Raman signals is usually small, and therefore it is crucial to further enhance the signals of Raman scattering. In this work, we demonstrate a low-cost and highly sensitive surface enhanced Raman scattering (SERS) substrate, which is comprised of the silicon nanowire (SiNW) array decorated with Au nanoparticles (AuNPs) on the surface and incorporated with a layer of Au backplane at the bottom, as shown in Fig. 1. Firstly, the SiNW array was prepared by a metal-assisted chemical etching (MaCE) method as a template of the SERS substrate. Then, the gold nanoparticles (AuNPs), which were successfully decorated on the surface of SiNWs array by an electron-beam evaporator under oblique angle deposition (OAD), enable localized surface plasmon resonance (LSPR) to substantially intensify the signal of Raman scattering from the analyte. Besides, we deposited an additional Au layer at the bottom of the SiNW array by electron-beam deposition under normal incidence. This additional Au layer, termed as a metal backplane (MBP), facilitates to reflect the back-scattered field rather than being absorbed by the silicon substrate, leading to the further enhancement of the SERS signals. Finally, the performance of this SERS substrate was optimized by a statistical Taguchi method. Our experimental verification indicates that for the analyte of 10^{-2} M self-assembled monolayer (S.A.M.) of thiophenol molecules, our tailored SERS substrate presents the average Raman signal up to1740 counts per second under a near infrared laser excitation (785 nm), which is 1.78 times stronger than a commercialized SERS substrate (Klarite®). Furthermore, our low-cost and high-sensitivity SERS substrate preforms reliably, showing a small coefficient of variation (C.V.) about 4.2%.

tjyen@mx.nthu.edu.tw

Waveguide-Embedded Modulator for Active Plasmonic Devices

Evgeniy Panchenko[1], Timothy James[1,2], Ann Roberts[1]
[1]*School of Physics, University of Melbourne, Melbourne, VIC, Australia*
[2]*(MCN), Melbourne Centre for Nanofabrication, Melbourne, VIC, Australia*

A major goal of active plasmonics is to create a device capable of modulating an input signal. Since surface plasmon polaritons (SPPs) are very sensitive to the properties of the surrounding media, changing the local permittivity of a plasmonic waveguide structure enables the modulation of the output signal. Moreover, the high field confinement permits performing the modulation on nanoscale dimensions.

Here we propose a modulator based on a metal-oxide-semiconductor (MOS) capacitor. Theoretical and experimental [1] studies of such structures have shown a satisfactory modulation depth per unit length at telecommunication wavelengths.

The plasmonic modulator presented here is designed to modulate the propagation of a fully plasmonic mode. The device is embedded on an insulator-metal-insulator (IMI) waveguide structure (FIG. 1) and consists of two metal slabs with dielectric and semiconductor layers between. We use an indium-tin oxide (ITO) as an active material in the modulator.

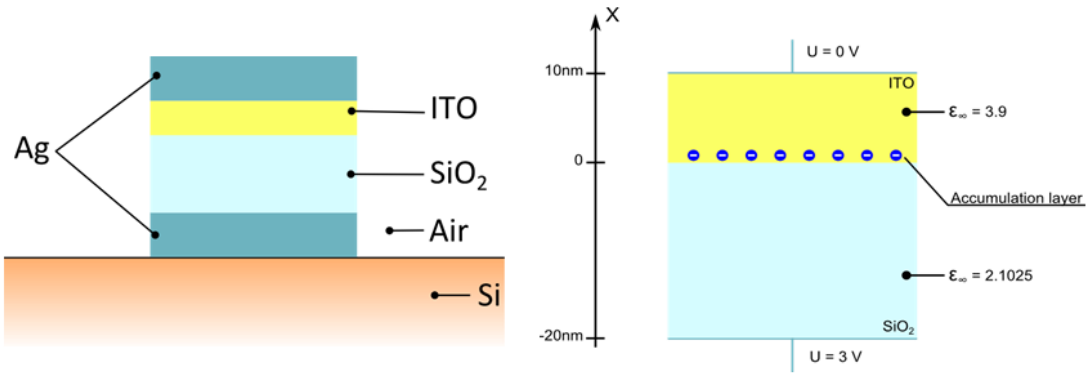

Applying an external potential to the metallic terminals leads to the accumulation of electrons at the ITO-SiO_2 interface. This in turn leads to a local change in the refractive index of the ITO layer. Moreover, the electric field strength inside the ITO layer increases which causes higher attenuation and, thus, a higher modulation depth.

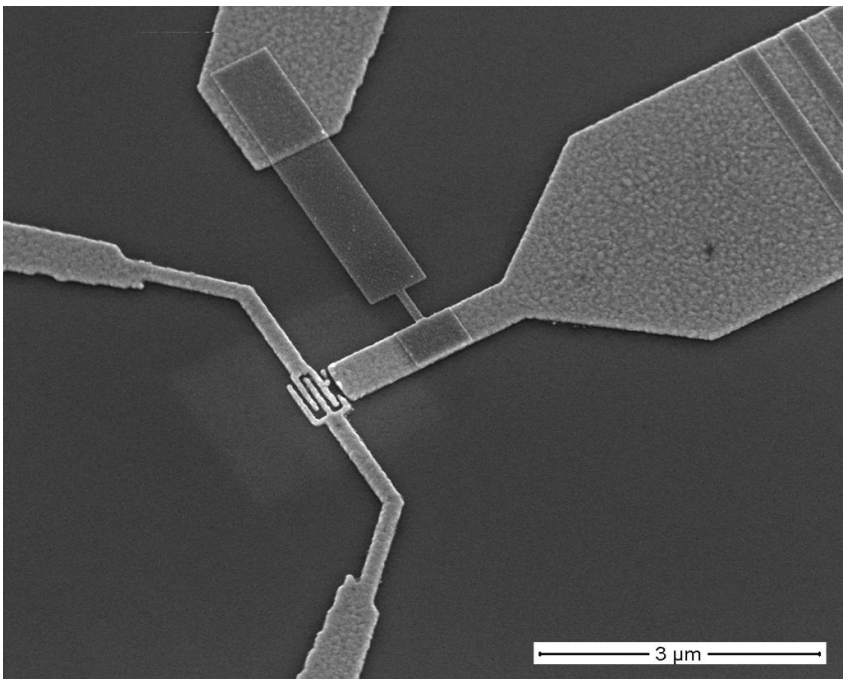

Also, due to the mismatch between the characteristic impedances of the MIM and IMI waveguides the modulator itself forms a Fabry-Perot resonator. This permits increasing the modulation depth even further, since the change of the ITO refractive index shifts the resonance and thus, increases reflection from the modulator.

Here we present theoretical and computational analysis of the plasmonic modulator. Progress in experimental studies of a fabricated device (FIG. 2) will also be presented.

References:

[1] Sorger, V *et al.*, Ultra-compact Silicon Nanophotonic Modulator with Broadband Response. Nanophotonics 2012, 1.1, 17-22

epanchenko@student.unimelb.edu.au

THz Plasmonic Filters created using a K-Space Design Technique

Andrew Paulsen, Ajay Nahata
Electrical and Computer Engineering, University of Utah, Salt Lake City, Utah, USA

The versatility and high performance of a wide range of filters enable the interconnected society we enjoy today. While well-defined filter design methodologies exist for much of the electromagnetic spectrum, the THz region of the spectrum lags behind in filter complexity. Various approaches to creating filters in the THz region have been shown [1]. While different types of filters have been demonstrated, an approach is still needed that can show versatility in designing arbitrary frequency responses within a single design methodology.

In this submission we show a THz filter design methodology based on k-space structures allowing for greater versatility in creating different classes of filters with one approach. In this design methodology the designer is free to define a desired frequency response which is then mapped into k-space. The k-space representation is then transformed into the spatial domain. We then fabricate the device using a conventional ink-jet printer with conductive silver ink and resistive carbon ink in which the grey scale image is converted to one in which the conductivity varies spatially.

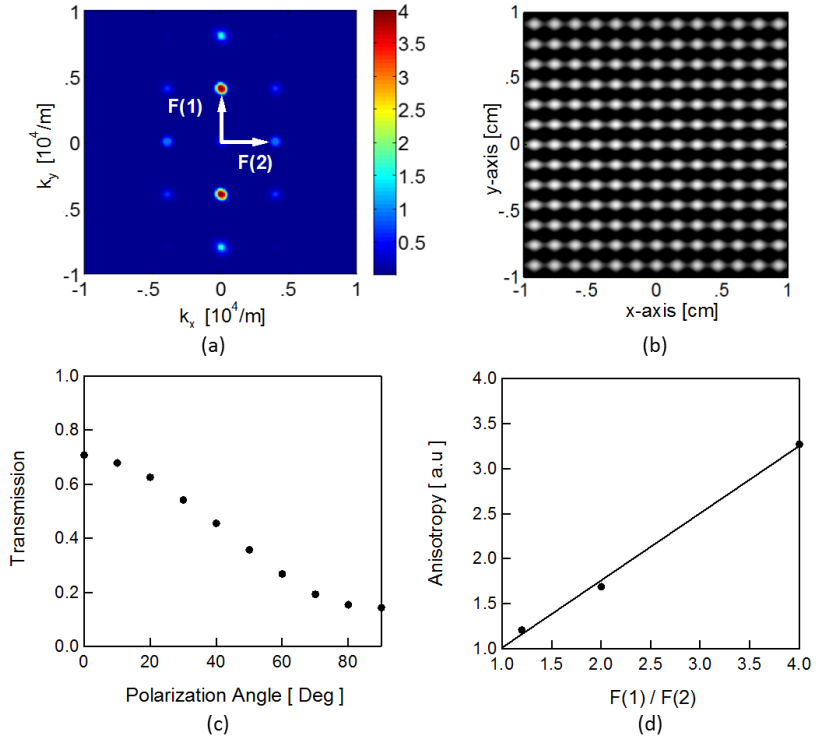

An example of such a filter is shown in Fig. 1, where the magnitude of F(1) and F(2) differ in k-space. The corresponding real space image (inverse Fourier transform of Fig. 1(a)) is shown in Fig. 1(b). The graph of absolute transmission at 0.18 THz versus the polarization of incoming radiation is shown in Fig. 1(c). Fig. 1(d) shows the anisotropy factor, which is the measured ratio of the magnitude of the resonance peaks for vertical and horizontal polarizations, respectively. A linear fit to the data shows that the measured anisotropy is in good agreement with the designed k-space anisotropy. This concept can be extended to other filter functionalities.

References

[1] A. M. Melo, et al., Adv. Opt. Technol. 2012

andrew.paulsen@utah.edu

Experimental Demonstration of Low Loss Gap Plasmon Waveguides on the Silicon-on-Insulator Platform

Michael Nielsen, Lucas Lafone, **Themistoklis Sidiropoulos**, Stefan Maier, Rupert Oulton
Physics, Imperial College London, London, UK

Facing the fundamental speed and integration limits of conventional semiconductor electronics, there has been a growing interest in developing all-optical circuitry capable of high speed broadband operation. Silicon photonics, due to its compatibility, was originally considered the obvious candidate. However, the optical diffraction limit restricts such photonic devices to minimum dimensions of half the operating wavelength, far in excess of those in conventional electronics. Here, silicon nanoplasmonics structures have been shown to be a viable alternative; these can operate in the sub-wavelength regime while still being capable of integration on a conventional electronic platform.

This work presents the first experimental demonstration of a novel silicon hybrid gap plasmon waveguide. Formed of a gap in a thin metal film atop an unetched silicon-on-insulator substrate, a recent theoretical proposal showed that these hybrid plasmonic waveguides had unique advantages for nanofocusing applications compared to other hybrid plasmonic waveguides [1]. At large gap widths, in excess of 100nm, the mode propagates primarily in the underlying silicon away from the metallic films, leading to propagation lengths in the tens or even hundreds of micrometres, with a 115nm Au gap having a demonstrated propagation length of 27μm at 1550nm. At these widths, the waveguides are ideal for long range low loss interconnect applications. When the waveguide width is focused much smaller than 100nm, the mode becomes concentrated in the gap, leading to mode areas far below the diffraction limit allowing for extreme nanofocusing. At extremely small gap widths, upwards of 90% of the modal power can be concentrated in the gap, albeit at the cost of reduced propagation lengths; a 25nm Au gap shows a propagation length of 4.5μm at 1550nm. In addition to measuring the linear propagation lengths of the waveguides, several common passive devices were designed, fabricated, and characterised based on these waveguides. Ideally, using a GaAs substrate, the strong focussing, and larger modal overlap with the substrate can be exploited to build sub-wavelength plasmonic nanolasers.

[1] L. Lafone, *et al.*, "Silicon-based metal-loaded plasmonic waveguides for low-loss nanofocusing.," Opt. Lett. **39**, 4356–9 (2014).

t.sidiropoulos10@imperial.ac.uk

Flexible Long-Range Plasmonic Waveguide for Tb/s Optical Interconnect Application

Christian Vernoux[1], Laurent Markey[1], Michael Nielsen[2], Sergey I. Bozhevolnyi[2], Thorsten Felder[3], Alain Dereux[1]
[1]*Nanosciences, Laboratoire Interdisciplinaire Carnot de Bourgogne UMR CNRS 6303, Dijon, France*
[2]*Institute of Technology and Innovation, University of Southern Denmark, Odense M, Denmark*
[3]*Momentive, Momentive Performance Materials GmbH, Leverkusen, Germany*

Flexible Long-Range SPP (LRSPP) have been proposed as possible components in datacom interconnect systems[1]. From the point of view of both processability and reliability the choice of the most convenient polymer to be used as cladding remains an issue. In the context of FP7 IP PHOXTROT, different polymers have been tested. Here we report on the LRSPP potential of Momentive's research materials. We fabricated LRSPP waveguides (typical Au cross-section 15nm x 10µm, cladding 10µm) after developing a fabrication process based on UV lithography and Au etching (Figure 1). The layers are built up successively onto a Si wafer from which the flexible waveguide can be detached later.

The samples were characterized by injecting TM-polarized light (1.55µm laser) from a single-mode fiber and observing the mode with an IR camera, in the top view and also transversally at the output facet for different waveguide widths (7.5, 10 and 12.5 µm). Figure 2 shows the mode observed at the output, in good agreement with the expected shape obtained from simulation, e.g. a 5x10µm ellipse for the 10µm-wide strip. A 14dB total insertion loss was measured for a 9mm length, corresponding to a ~3mm SPP propagation length. The measured bending losses will also be presented.

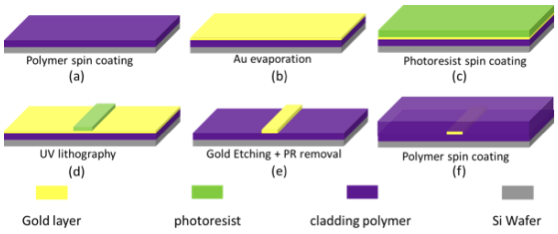

Figure 1: LR-SPP waveguide fabrication

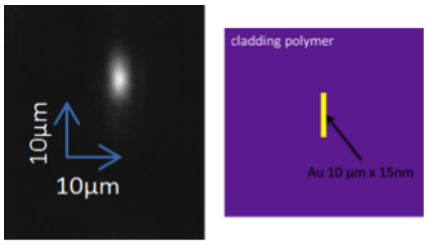

Figure 2: Output LR-SPP mode imaged at 1.55µm (left) ; corresponding structure (right).

[1] Jong-Moo Lee, *al*. Opt. Express, 17(1), 228–234 (2009).

christian.vernoux@u-bourgogne.fr

Visible Light Modulation with Graphene

Renwen Yu, Javier F. García de Abajo
Nanophotonics theory, The Institute of Photonic Sciences, Castelldefels, Spain

Fast modulation and switching of light at visible and near-infrared (vis-NIR) frequencies is of utmost importance for optical signal processing and sensing technologies. No fundamental limit appears to prevent us from designing wavelength-sized devices capable of controlling the light phase and intensity at terahertz speeds in those spectral ranges. However, this problem remains largely unsolved, despite recent advances in the use of quantum wells and phase-change materials for that purpose.

Here, we explore an alternative solution based upon the remarkable electro-optical properties of graphene. In particular, we predict unity-order changes in the transmission and absorption of vis-NIR light produced upon electrical doping of graphene sheets coupled to realistically engineered optical cavities. The light intensity is enhanced at the graphene plane, and so is its absorption, which can be switched and modulated via Pauli blocking through varying the level of doping. Specifically, we explore dielectric planar cavities operated under resonant tunneling transmission conditions, as well as Mie modes in silicon nanospheres and lattice resonances in metal particle arrays. Our simulations reveal absolute variations in transmission ~ 90% using feasible material parameters, thus supporting the use of graphene for fast electro-optics at vis- NIR frequencies.

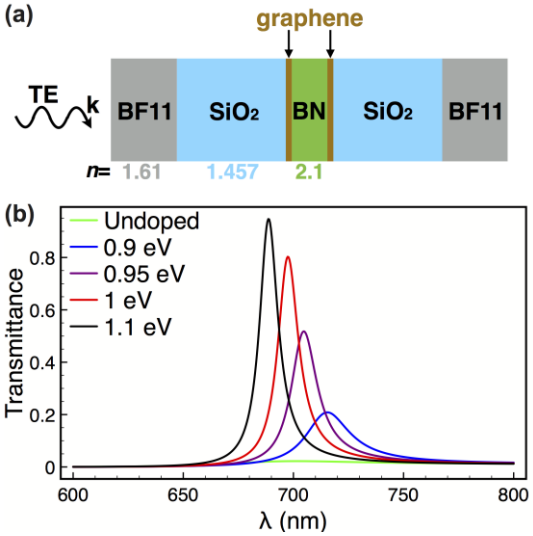

We present a planar multilayer structure considered for resonant tunneling light transmission, including a central BN planar waveguide (not to scale) and two single-layer graphene films intercalated at the BN/SiO2 interfaces. We show that transmission spectra of the multilayer structure at an incidence angle of 71 degrees for different levels of doping. At a wavelength of 689 nm, transmittance can be tuned from 95% to almost 0.

References

[1] R. Sainidou, et al., Nano Lett 10, 4450 (2010).

[2] F. J. García de Abajo, Acs Photon. 1, 135 (2014).

renwen.yu@icfo.es

Experimental Demonstration of CMOS-Compatible Long-Range Dielectric-Loaded Surface Plasmon-Polariton Waveguides (LR-DLSPPWs)

Roy Zektzer[1], Boris Desiatov[1], Noa Mazurski[1], Sergey I. Bozhevolnyi[2], Uriel Levy[1]

[1]*Applied Physics, The Hebrew University of Jerusalem, Jerusalem, Israel*

[2]*Department of Technology and Innovation, University of Southern Denmark, Odense, Denmark*

A major obstacle of plasmonic waveguides [1-2] is their limited propagation length. Hybrid photonic-plasmonic waveguides were proposed and demonstrated, providing longer propagation length at the expense of weaker mode confinement [3]. Specifically, the long-range dielectric-loaded surface plasmon-polariton waveguide (LR-DLSPPW) [4] offers decent propagation length together with wavelength scale mode confinement. By generating a symmetric-like dielectric environment above and below a thin metal stripe, a long range mode is supported [5]. In this work we demonstrate the design, fabrication and experimental characterization of a high refractive index, CMOS compatible LR-DLSPPWs. The LR-DLSPPW configuration is designed to operate around 1.55 micron wavelength. Our LR-DLSPPW (Fig. 1) consists of a Si_3N_4 ridge deposited on top of a thin aluminum (Al) strip, which is supported by oxidized silicon-on-insulator (SOI) wafer. Figure.1 (a) presents simplified schematics of the device configuration, while Fig. 1(b) shows the device geometry, which is the result of our fabrication process as can be seen in the SEM image (Fig. 1(c)).

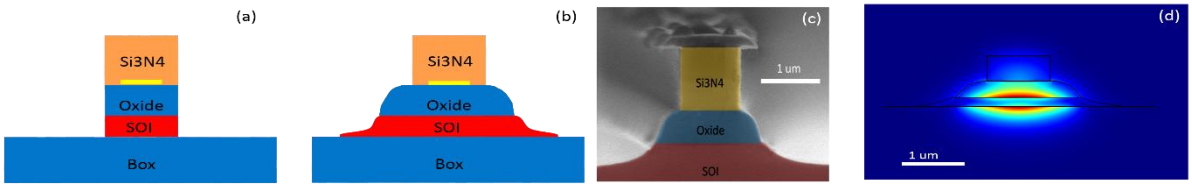

From spectral transmission measurements we have concluded that the propagation loss of the fundamental LR-DLSPPW mode (Fig. 1(d)) is ~6 dB/mm, which is comparable to previously published results, with the estimated mode confinement being ~0.5mm^2. Furthermore, we have measured the mode profile using a near field scanning optical microscope (Fig. 2). The near field data show a beat pattern, from which we extract the effective indices of the two modes supported by the structure. The results will be reported in details and discussed during the presentation. We will also point out further research opportunities which can be supported by the reported waveguide platform.

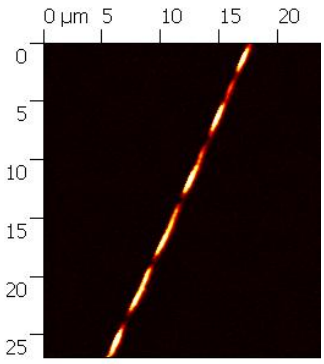

K. Gramotnev and S. I. Bozhevolnyi, "Plasmonics beyond the diffraction limit," Nat. Photonics **4**, 83-91 (2010).

I. Bozhevolnyi, V. S. Volkov, E. Devaux, J.Y. Laluet, and T. W. Ebbesen, "Channel plasmon subwavelength waveguide components including interferometers and ring resonators," Nature 440, 508-511 (2006).

Goykhman, B. Desiatov, and U. Levy, "Experimental demonstration of locally oxidized hybrid silicon-plasmonic waveguide," Appl. Phys. Lett. **97**(14), 141106 (2010).

S. Volkov, Z. Han, M. G. Nielsen, K. Leosson, H. Keshmiri, J. Gosciniak, O. Albrektsen, and S. I. Bozhevolnyi, "Long-range dielectric-loaded surface plasmon polariton waveguides operating at telecommunication wavelengths," Opt. Lett. **36**(21), 4278–4280 (2011).

Sarid "Long-Range Surface-Plasma Waves on Very Thin Metal Films," Phys. Rev. Lett. **47**, 1927-1930 (1981).

roy.zektzer@mail.huji.ac.il

Low-Loss, Fabrication-Tolerant, TM-Pass Polarizer Based on Hybrid Plasmonic Waveguide

Zhiping Zhou, Linfei Gao
Electronics, Peking University, Beijing, China

Plasmonics has a potential to help the miniaturization and integration of the photonic devices for telecommunications. However, its practical usage has always been controversial because the plasmon photonic devices are usually lossy and difficult to fabricate. One promising approach is hybrid integration that using plasmonics in functional devices and dielectrics for propagation and connection.

Over the past years, our group has developed a series of novel approaches and constructed a few compact and practical plasmon photonic devices for telecommunications, such as wavelength demultiplexing [1], Band-pass plasmonic slot filter [2], polarization beam splitters [3], and polarization rotators [4]. Polarization handling is an essential issue in telecommunication [5]. While traditional polarization handling devices using dielectric structures which have large size or complicated geometries, we believe that plasmonics, with natural polarization sensitivity and good confinement, will surely help to develop better devices for telecommunication.

Here we propose a low-loss, fabrication-tolerant, and compact TM-pass polarizer based on hybrid plasmonic waveguide (HPW). As shown in Fig. 1, a narrow HPW (consists of Si wire, SiO_2 gap and metal cap) as the polarizer is seamless connected with standard Si wire input/output waveguides through taper couplers. At a small Si width, TE mode in HPW is cut off while TM mode still survives because its plasmonic property. Therefore, the narrow HPW acts as a TM-pass filter. Notably, the metal strip here is wider than Si wire and can be alignment-free during the fabrication, avoiding the biggest challenge in traditional HPW that requires precise alignment between metal and Si waveguide. Moreover, wider metal helps increase TE mode loss and reduce TM mode loss, thus enhances extinction ratio (ER). Fig. 2 and 3 show the simulation results of a 4 μm-long device, from which we obtain ER is higher than 18 dB, while TM insertion loss is only 0.66 dB. The experiment is underway and we expect to show the results at the conference.

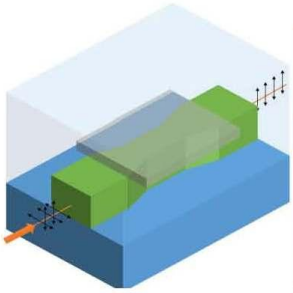

Fig. 1 3D schematic of the device

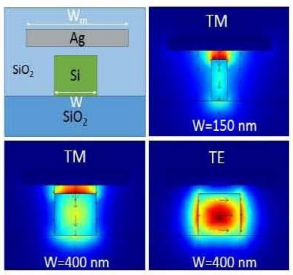

Fig. 2 Cross section of HPW and normalized E field distribution

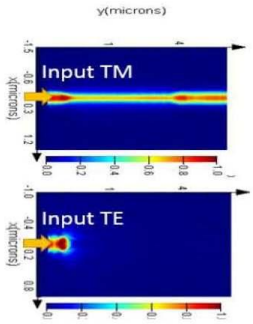

Fig. 3D FDTD simulation.Power distribution when input TM and TE respectively

References

[1] F Hu, H Yi, Z Zhou, Optics letters 36 (8), 1500-1502

[2] F Hu, H Yi, Z Zhou, Optics express 19 (6), 4848-4855

[3] L. Gao, Z. Zhou, et al, Appl. Phys. B, 113, 199, 2013

[4] L. Gao, Y. Huo, J. S. Harris and Z. Zhou, IEEE Photonic. Tech. Lett., 25, 2081, 2013

[5] T. Barwicz, H.I. Smith, et al, Nat. Photonics,1, 57, 2007

zjzhou@pku.edu.cn

Self-Referenced Meaurements of the Terahertz Dielectric Properties of Metals via Excitation of Surface Plasmon-Polaritons

Shashank Pandey, Barun Gupta, **Ajay Nahata**
Department of Electrical and Computer Engineering, University of Utah,
Salt Lake City, Utah, USA

It is generally accepted that the terahertz (THz) dielectric properties of conventional metals are orders of magnitude larger than at optical frequencies. This is based on an extrapolation using the Drude model [1] and has led to the general view that metals can be approximated at perfect electrical conductors (PECs) in the long wavelength regime.However, the PEC approximation yields results that deviate from experimental results. For example, the predicted 1/e out-of-plane decay length for surface plasmon-polaritons (SPP) on unstructured metal films is on the order of ten cm based on the published dielectric data, while experimental measurements typically yield values on the order of a few mm [2].

Here, we show unambiguous measurements of the THz permittivity of several different conventional metals using a modified THz time-domain spectrometer, shown in Fig.1, that does not require a "perfect reference."

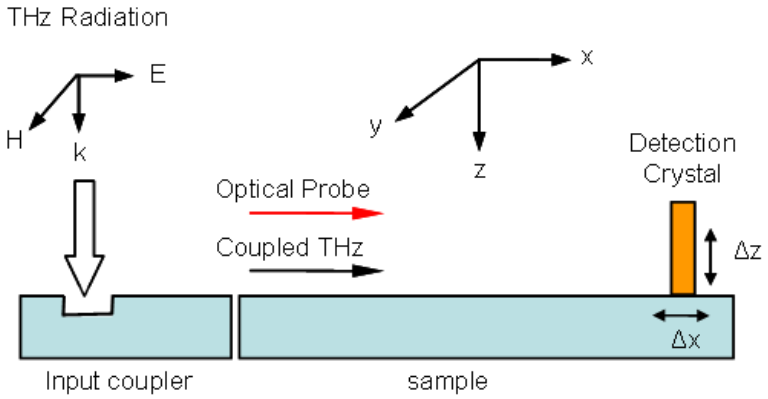

We measure the complete time-domain electric field information at several different locations along the x axis and use that information to calculate the metal permittivity. Independently, we measure the 1/e decay lengths along both the x and z-axes and compare that to the values associated with the measured permittivity. In Fig.2, we show the 1/e propagation length along the x-axis for gold based on published dielectric data, from measured dielectric values and from direct measurements [3].

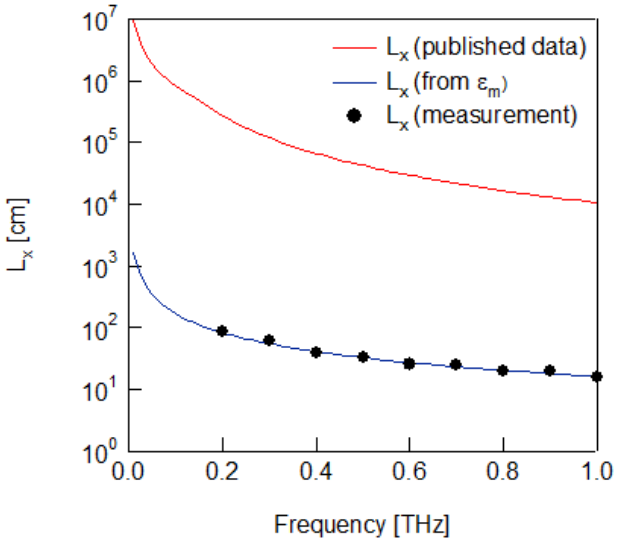

References

[1] M. A. Ordal, et.al., Appl. Opt. **22**, 1099–1119 (1983).

[2] T.I. Jeon and D. Grischowsky, Appl.Phys.Lett. **88**, 061113 (2006).

[3] S.Pandey, S.Liu, B.Gupta and A.Nahata, Photon. Res. **1**,4, (2013).

ajay.nahata@utah.edu

Nanofocusing of Ultraviolet Light in Aluminum V-Grooves

Jieying Mao[1], **Steve Blair**[2]
[1]*Department of Physics and Astronomy, University of Utah, Salt Lake City, Utah, USA*
[2]*Department of Electrical and Computer Engineering, University of Utah, Salt Lake City, Utah, USA*

As significant progress has been accomplished in visible and infrared nanofocusing, the study of Ultraviolet (UV) plasmons are attracting interest due to their numerous applications such as label free detection of biological molecules. In this work, electromagnetic nanofocusing of UV light incident upon Aluminum (Al) V-groove nanostructures is simulated using the finite-difference time-domain (FDTD) method. A parametric study of the field enhancement around the V-groove tip area is conducted through the change of groove depth, width, and the tip angle. A short-wavelength threshold of about 200 nm, lying well above the plasma wavelength of Al, is identified, below which the electric field enhancement at the tip rapidly decreases. The adiabatic focusing condition and mode attenuation are taken into consideration as possible explanations. Through simplification of the V-groove model into a Metal-Dielectric-Metal (MDM) waveguide with gap width corresponding to V-groove width (based upon distance from the tip), modal solutions can be obtained for the complex propagation constant, from which the adiabatic parameter and propagation length are determined. These results suggest that the decrease in propagation length with decreasing wavelength is the underlying cause of the short-wavelength threshold.

References

[1] D. K. Gramotnev, J. Appl. Phys. 98, 104302 (2005).

[2] D. F. P. Pile, Appl. Phys. B: Laser Opt. 81, 607 (2005).

[3] D. F. P. Pile and D. K. Gramotnev, Appl. Phys. Lett. 89, 041111 (2006).

[4] D. K. Gramotnev and D. F. P. Pile, Appl. Phys. Lett. 85, 6323 (2004).

[5] M. I. Stockman, Phys. Rev. Lett. 93, 137404 (2004).

[6] M. W. Vogel and D. K. Gramotnev, Phys. Lett. A 363, 507511 (2007).

[7] R. F. Chen, Anal. Lett. 1, 3542 (1967).

[8] C. R. Johnson, M. Ludwig, S. ODonnell, and S. A. Asher, J. Am. Chem. Soc. 106, 50085010 (1984).

[9] K. Ray, M. H. Chowdhury, and J. R. Lakowicz, Anal. Chem. 79, 64806487 (2007).

[10] P. R. West, S. Ishii, G. V. Naik, N. K. Emani, V. M. Shalaev, and A. Boltasseva, Laser & Photon. Rev. 4, 795808 (2010).

Blair@ece.utah.edu

Surface Waves on Hyperbolic Metasurface

Oleg Yermakov[1], Anton Ovcharenko[1], **Andrey Bogdanov**[1,2], Ivan Iorsh[1]
[1]*The International Research Centre for Nanophotonics and Metamaterials, ITMO University, St Petersburg, Russia*
[2]*Theoretical Bases of Microelectronics, Ioffe Institute, St Petersburg, Russia*

In this work we analyze new type of surface electromagnetic waves which can propagate along hyperbolic metasurface (Fig.1a), i.e. along the plane layer which can be described by a conductivity tensor with indefinite signature ($\mathrm{Im}(\sigma_{\parallel})$ $\mathrm{Im}(\sigma_{\perp})0$). We propose that $\sigma_{\parallel}$ and $\sigma_{\perp}$ have Drude-Lorentz dispersion with resonant frequencies $\Omega_{\parallel}$ and $\Omega_{\perp}$ (Fig.1b). Therefore, regime of hyperbolic metasurface is realized in the range $\Omega_{\perp}\omega\Omega_{\parallel}$. We have shown that there are two surface waves of hybrid TE-TM polarization which can propagate along the metasurface. Their dispersion for different propagation angles α is shown in Fig.1c.

Equal frequency contours, optical losses and electromagnetic field distribution are analyzed in detail. The analysis showed that the surface waves have unusual polarization properties and have common features with Dyakonov surface waves [M.I. Dyakonov, JETP 67, 717 (1988)] and magnetoplasmons [K. W. Chiu and J. J. Quinn, Phys. Rev. B 9, 4724 (1974)].

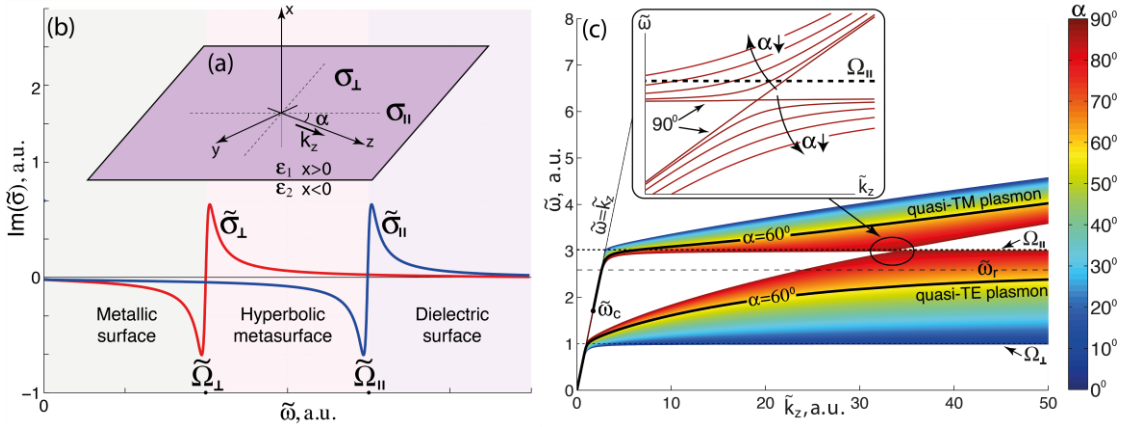

Fig.1 (a) Hyperbolic metasurface separating two dielectric media. Conductivities $\sigma_{\parallel}$ and $\sigma_{\perp}$ correspond to the principle axes of the conductivity tensor. (b) Conductivities $\sigma_{\parallel}$ and $\sigma_{\perp}$ have Drude-Lorentz dispersion with resonance frequencies $\Omega_{\parallel}$ and $\Omega_{\perp}$. α is the angle between wavevector k_z and principle axis of the conductivity tensor corresponding to $\sigma_{\parallel}$. (c) Dispersion of surface waves depending on propagation angle α.

bogdan.taurus@gmail.com

Surface Plasmon Enhanced Photoluminescence from Copper Nanoparticles: Influence of Temperature

Illya Bondarchuk, Yeshchenko Oleg, Losytskyy Mykhaylo
Department of Physics, Taras Shevchenko National University of Kyiv, Kyiv, Ukraine

Anomalous temperature dependence of surface plasmon enhanced photoluminescence from copper nanoparticles embedded in a silica host matrix has been observed. The quantum yield of photoluminescence increases as the temperature increases. The key role of such an effect is the interplay between the surface plasmon resonance and the interband transitions in the copper nanoparticles occurring at change of the temperature. Namely, the increase of temperature leads to the red shift of the resonance. The shift leads to increase of the spectral overlap of the resonance with photoluminescence band of copper as well as to the decrease of plasmon damping caused by interband transitions. Such mechanisms lead to the increase of surface plasmon enhancement factor and, consequently, to increase of the quantum yield of the photoluminescence.

illya.posv.b@gmail.com

Investigation of Interaction and Rabi Splitting of Surface and Localized Plasmons by Ellipsometry

Eugene Bortchagovsky[1], Alla Bogoslovskaya[2]
[1]*31, Institute of Semiconductor Physics of NAS of Ukraine, Kiev, Ukraine*
[2]*12, Institute of Semiconductor Physics of NAS of Ukraine, Kiev, Ukraine*

It is well known that two interacting resonances hybridize and split producing energy gap between two hybridized modes instead of two independent resonances. Different parameters of interacting systems play role in the determination of such a splitting. The most popular system for the investigation of such an interaction is a molecular layer on the surface of a metal supporting surface plasmon [1]. Regulating the distance between the layer with molecular exciton and the surface allows to control the strength of the exciton-plasmon interaction. However bleaching and no possibility to regulate parameters for chosen molecules restrict the flexibility of such investigations. The exchange of the layer of molecules by nanoparticles possessing localized plasmon makes such a system more convenient for investigations. Possibilities to manage parameters of localized plasmon by size, shape and the concentration of nanoparticles opens new perspectives for such a task.

Spectroscopic investigations of such a system were already reported [2]. In the present work we used ellipsometry to check plasmonic interactions. Ellipsometry is a method, which allows to register plasmon resonance position and to monitor not only amplitude but phase information too. The latter is important for the reconstruction of the whole picture of the interaction and splitting as well as allows to obtain information about near-field local interactions from parameters of far field. Obtained results clearly demonstrate splitting of resonances and different effectiveness of the energy transfer at different angles of incidence. We hope the simultaneous registration of amplitude and phase characteristics of resonances would allow to reveal the spectral shift between near-field and far-field resonances.

[1] P. Törmä and W.L. Barnes, Rep. Prog. Phys. submitted.

[2] A. Rueda, M. Stemmler, R. Bauer, Yu. Fogel, K. Müllen, and M. Kreiter, J Phys Chem C **112** (2008) 14801.

bortch@yahoo.com

Depolarization of Light at the Frequency of Localized Surface Plasmon Resonance as the Probe of Interparticle Interaction

Eugene Bortchagovsky[1], Tetiana Mishakova[2]
[1]*31, Institute of Semiconductor Physics of NAS of Ukraine, Kiev, Ukraine*
[2]*Institute of High Technology, Taras Shevchenko National University of Kiev, Kiev, Ukraine*

Spectroscopic ellipsometry with the account of depolarization applied for few disordered layers of nanoparticles demonstrated different level of depolarization at the frequency of the localized plasmon depending on the temperature of annealing. The temperature of annealing higher the level of depolarization lower. Scanning electron microscopy revealed the shape and size distribution of nanoparticles, which approaches the layer of practically round nanoparticles produced at highest annealing temperature and rather shapeless particles for lowest annealing temperature.

We speculate that for the creation of depolarized light scattered by the layer of nanoparticles the energy of localized plasmon should be stored and the excitation should be dephased in some noninstant process. We propose the model of the Forster energy transfer between plasmons localized at different nanoparticles as such a process. This process can easily create dephasing at the energy migration and storing. Additionally such a transfer should be greatly enhanced at the frequency of the resonance as it is proportional to the multiplication of dipole moments of participating particles what we observe in the experiment.

At the same time, only dephasing is not enough for the creation of depolarization as even completely incoherent light may be totally polarized. It is the particle shape, which can give us the necessary disorientation of dephased dipoles. If all particles are round the direction of the excitation at the resonance frequency is degenerated. In such a case the transferred excitation would have the same orientation of the dipole moment as the initial one, so all scattered light will keep the polarization. The opposite situation is for shapeless particles. In this case the dipole moment of the resonance of the acceptor may be disoriented according to the dipole moment of the resonance of the donor, what gives the second necessary element for the creation of depolarization.

bortch@yahoo.com

Strong Electron - Plasmon Interaction in Scanning Electron Microscopy

Moshik Cohen[1,2], Yossi Abulafia[2], Zeev Zalevsky[1,2]
[1]*Faculty of Engineering, Bar-Ilan University, Ramat-Gan, Israel*
[2]*Bar-Ilan Institute for Nanotechnology & Advanced Materials, BINA, Ramat-Gan, Israel*

Nanoplasmonics has fashioned rapid expansion of interest from both fundamental and applicative perspectives, with potential for becoming a true life – changing technology[1–3]. However, fundamental and practical limitations impede plasmonic technology from fulfilling its potential. This includes nanofabrication inaccuracies, difficulties in delivering light to nanoscale devices and nanocharacterization complexities.

Here, for the first time, we address these limitations by performing *simultaneous* excitation, nanoimaging and functional characterization of plasmonic devices using scanning electron microscopy (SEM). We use a high-energy (50KeV), focus(1nm) electron beam to excite optical plasmonic modes in nanometallic devices.

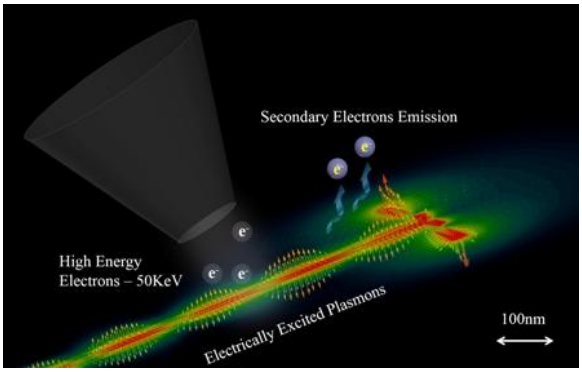

Figure 1| Illustration of plasmonic excitation and nanoimaging with SEM. Dipole nanoantenna is connected to MIM waveguide. The device is illuminated by a high energy scanning electron beam, which excites optical plasmons in the device.

We analyze the emitted electrons to obtain the broadband optical response and the geometrical topography of the devices. Our approach achieves optical characterization and topography imaging, both with deep subwavelength spatial resolution of only 30nm. High resolution images that include both topography and functional information are created within less than 10 seconds. Our experimental results are in good agreement with full wave numerical calculations, and supported by an analytic model for increased physical insight.

Our findings enable rapid prototyping of nanoplasmonic devices operating at optical frequencies. It will now be possible to accurately deliver high energy to nanoscale geometries, and precisely analyze their response via electron - plasmon interaction.

References

Cohen, M., Shavit, R. & Zalevsky, Z. Observing Optical Plasmons on a Single Nanometer Scale. Sci. Rep. 4.(2014).

Cohen, M., Zalevsky, Z. & Shavit, R. Towards integrated nanoplasmonic logic circuitry. Nanoscale 5, 5442–5449 (2013).

Brongersma, M. L. & Shalaev, V. M. The Case for Plasmonics. Science 328, 440–441.(2010).

moshik.cohen80@gmail.com

Observation of Giant Vacuum Rabi Splitting in Complexes of Aluminum Nanoantennas and J-Aggregates and Generation of Polarized Hybrid States

Elad Eizner, Ori Avayu, Tal Ellenbogen
Department of Physical Electronics, Fleischman Faculty of Engineering, Tel Aviv University, Tel Aviv, Israel

In recent years several works studied the formation of hybrid exciton-localized-surface-plasmon (X-LSPs) modes in various material systems [1-3], and demonstrated that these modes enable different interesting nanoscale control schemes, e.g, ultra-fast all-optical switching [4]. Up to date X-LSPs were mainly studied using silver or gold as the plasmonic material however here we demonstrate that aluminum is also well suited for strong coupling experiments and enable the generation of X-LSPs across the entire visible spectrum potentially down to the ultraviolate regime. Despite the relatively high damping rates of aluminum we observe in our experiments a giant Rabi splitting of more than 400 meV. In addition we show that the coupling of vacuum LSP flactuations with the excitons can be polarized by geometrical manipulations of the nanoantennas. This opens new possibilities to study the dynamics of strongly coupled plasmon-exciton states.

The studied samples consist of aluminum nanodisks or nanorods arrays on indium tin oxide coated glass substrate. An SEM image of one of the nanodisks arrays is shown in Figure 1(a) and an image of arrays transmission, exhibiting vivid colors can be seen in Figure 1(b). Figure 1(c) shows the transmission spectra of the nanodisks arrays. In each array, nanodisks are 40 nm high with different diameter, separated by 190 nm side to side. The samples are then spin coated with a thin layer of TDBC J-aggregating dyes in water. This leads to the emergence of hybrid X-LSP states as can be seen from the anti-crossing in the dispersion measurements shown in Figure 1(d) (nanodisks) or 1(e) (nanorods). Nanorods arrays consist of 40 nm high, 40 nm wide nanorods with different lengths, separated by 190 nm side to side at their long axis and 150 nm side to side at their short axis. As can be seen from Figure 1(f), when the shined light is polarized with the short axis of the nanorods we observe only the uncoupled J-aggregate dyes absorption.

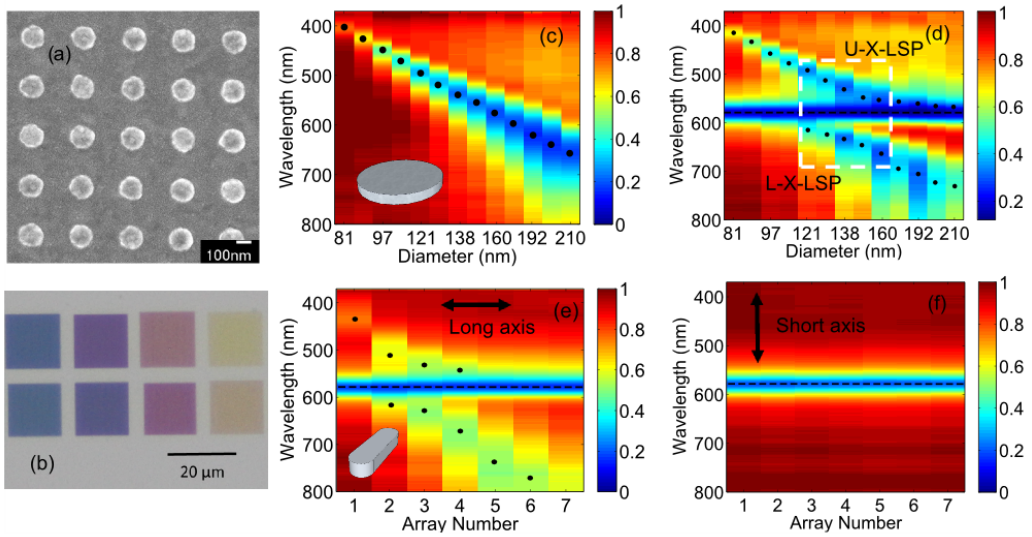

[1] J. Bellessa et al. Phys. Rev. B 80, 033303 (2009).

[2] A. E. Schlatheret et al. Nano. Lett. 13, 3281–6 (2013).

[3 P. Chantharasupawong et al. J. Phys. Chem. C 118 (41), 23954 (2014).

[4] P. Vasa et al. ACS Nano 4, 7559–7565 (2010)

eladeiz@post.tau.ac.il

Probing Nanographene Phonons with Electron Energy-Loss Spectroscopy

Martinez Saavedra Jose Ramon[1], J. Lopez[1], Javier F. García de Abajo[1,2]
[1]*Nanophotonics Theory, ICFO - The Institute of Photonic Sciences, Castelldefels, Barcelona, Spain*
[2]*ICREA - Institucio Catalana de Recerca i Estudis Avançats, Barcelona, Spain*

Electron energy-loss spectroscopy (EELS) performed on transmission electron microscopes (TEMs) is widely used for the characterization of optical excitations with atomic resolution [1,2]. The energy of the electrons ~100 keV`s makes it difficult to resolve very low frequency excitations, such as phonons. High-resolution EELS (HREELS) offers an alternative that is capable of resolving molecular adsorption [3] and surface vibrations [4] using less energetic electrons, although this technique lacks spatial resolution below a few nanometers. Recent developments in TEMs have pushed the energy resolution down to ~10 meV [5], thus enabling the study of optical phonons with atomic resolution.

Stimulated by these experimental advances, we theoretically study the high frequency vibrational modes of nanographene structures and extended graphene layers. We discuss both loss spectra and spatially resolved maps for different structures and compare them with the local density of acoustic (or vibrational) states (LDAS), showing how optical phonons can be sampled and studied by means of the new electron microscopes (see Fig. 1). We further discuss the origin of the different features in the spectra, as originating from specific vibrational modes of the structures. The limit of extended graphene is smoothly recovered for large structures. We predict large inelastic signal intensities due to the divergent character of the electron-sample interaction at low frequencies, thus anticipating that phonon losses will produce observable signals down to samples of molecular size.

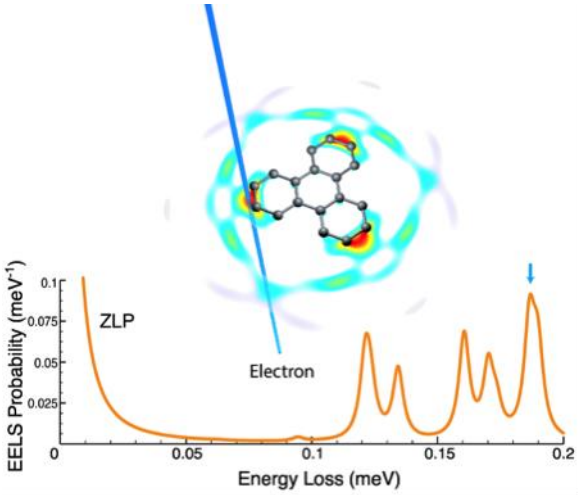

References

[1] Egerton, R.F., *Electron energy-loss spectroscopy in the electron microscope*, Springer (1996).

[2] García de Abajo, FJ, Rev. Mod. Phys. **82**, 209-275 (2010).

[3] Whang, E.K. *et al.*, Phys. Rev. B **63**, 075401 (2001) .

[4] Ibach, H., Mills, D.L., *Electron energy-loss spectroscopy and surface vibrations*, Academic Press (1982).

[5] Krivanek, O.L., *et al*, Nature **514**, 209-212 (2014).

jose.martinez@icfo.es

Mapping of Plasmonic Modes in Gold Nanoparticles by Means of Electron Energy Loss Spectroscopy

Vlastimil Křápek[1], Ai Leen Koh[2], Lukáš Břínek[1,3], Martin Hrtoň[1,3], Ondřej Tomanec[3,4], Radek Kalousek[1,3], Stefan Maier[5], Tomáš Šikola[1,3]

[1]*Central European Institute of Technology, Brno University of Technology, Brno, Czech Republic*

[2]*Stanford Nano Shared Facilities, Stanford University, Stanford, USA*

[3]*Institute of Physical Engineering, Brno University of Technology, Brno, Czech Republic*

[4]*Faculty of Science, Palacký University, Olomouc, Czech Republic*

[5]*Department of Physics, Imperial College London, London, UK*

In metallic nanoparticles, collective oscillations of free electron plasma strongly couple to the electromagnetic field forming the excitations called localized surface plasmons (LSP). A characteristic feature of LSP is a strong enhancement of electromagnetic field within the surrounding dielectric together with its confinement on the subwavelength scale, which can be utilized to control various optical processes in the visible and near infrared spectral region. For example, a plasmonic particle attached to an optical emitter can be used to enhance the absorption of the exciting radiation, amplify or quench the spontaneous emission rate of the emitter, directing the emitted light or as a coupler for a waveguide in integrated optical circuits.

Electron energy loss spectroscopy (EELS) is a method allowing to study both the spatial and spectral distribution of LSP resonances. The electron beam with a narrow kinetic energy distribution passes through or close to the metallic nanoparticle and induces LSP excitations, whose electric field in turn scatters the electrons inelastically. Scanning the sample and recording the energy loss spectrum at each position allows to infer the LSP properties.

In our contribution we present EELS study of gold crescent-shape nanoparticles. These structures exhibit particularly large field enhancement near their sharp features, support two non-degenerate dipolar (i.e., optically active) LSP resonances and are widely tunable. Depending on the volume and shape, we resolved up to four LSP resonances in every metallic particle in the energy range 0.8 – 2.4 eV. The boundary element method calculations helped to identify the character of the resonances and showed that the highest energy feature is a multi-resonance assembly. The two lowest resonances are of importance due to their dipolar character. Remarkably, they are both concentrated near the tips of the crescent, spectrally well resolved and their energies can be tuned between 0.8 – 1.5 eV and 1.2 – 2.0 eV, respectively. As the lower spectral range covers the telecom wavelengths 1.3 and 1.55 μm, we envisage the use of such nanostructures in infrared communication technology.

vlastimil.krapek@ceitec.vutbr.cz

Simultaneous Experimental Observation of the Quantization and the Interference Pattern of a Plasmonic Near-Field

Tom Lummen[1], Luca Piazza[1], Erik Quiñonez[2], Yoshie Murooka[1], Bryan Reed[3], Brett Barwick[2], Fabrizio Carbone[1]
[1]*Laboratory for Ultrafast Microscopy and Electron Scattering, École Polytechnique Fédérale de Lausanne, Lausanne, Vaud, Switzerland*
[2]*Department of Physics, Trinity College, Hartford, Connecticut, USA*
[3]*Physical and Life Sciences Directorate, Lawrence Livermore National Laboratory, Livermore, California, USA*

Miniaturized plasmonic and photonic integrated circuits are generally considered as the core of future generations of optoelectronic devices, due to their potential to bridge the size-compatibility gap between photonics and electronics. However, as the nanoscale is approached in increasingly small plasmonic and photonic systems, the need to experimentally observe and characterize their behavior in detail faces increasingly stringent requirements in terms of spatial and temporal resolution, field of view, and acquisition time. This work focuses on a specific electron microscopy technique, Photon-Induced Near-Field Electron Microscopy (PINEM), which is capable of imaging optical evanescent fields and surface plasmon polaritons (SPPs) in nanoplasmonic structures with both nanometer and femtosecond resolution. To do so, an advanced electron energy filter is used to analyze the quantized energy exchange between a photo-induced SPP and an ultra-short bunch of probing electrons. In electron energy loss/gain spectroscopy mode, the exchange of up to 30 photon quanta with the photo-induced SPPs in silver nanoantennae is observed. In PINEM imaging mode, the spatial properties of the photo-induced standing SPP wave on a single silver nanoresonator are shown to be controlled by the polarization of the optical pump pulse. These results are guided and corroborated by extensive 3D finite-element modeling. Moreover, in a novel hybrid acquisition mode - which synchronously characterizes the electron-SPP interaction along both a spatial coordinate and energy - both the characteristic spatial interference and the energy quantization of the SPP are obtained in the same experiment, providing a unique visualization of the wave-particle duality of its electromagnetic near-field.

tom.lummen@epfl.ch

Influence of Temperature on Photoluminescence of Rhodamine 6G in Plasmonic Field of Gold Nanoparticles

Oleg Yeshchenko, Illya Bondarchuk, Viktor Kozachenko, Mykhaylo Losytskyy
Physics Department, Taras Shevchenko National University of Kyiv, Kyiv, Ukraine

The comparative study of the temperature dependence of the photoluminescence (PL) from rhodamine 6G (R6G) deposited on 2D array of gold nanoparticles (NPs) and PL from R6G without Au NPs was performed in the temperature range of 78 – 298 K. The PL from R6G on Au NPs array is enhanced by the coupling of exciting and emitted photons to the surface plasmons excited in the NPs. There is a significant difference in the temperature behavior of the PL spectra from R6G–Au and R6G samples. The ratio of PL intensity of R6G on Au to one of R6G without Au was found to be monotonically decreasing with temperature. This indicates the fact of monotonic decrease of the factor of plasmonic enhancement of PL from R6G on Au NPs with temperature. The theoretical model was proposed to explain the observed temperature dependence of plasmonic enhancement factor. Two possible physical mechanisms of the observed temperature dependence were considered. First one is the electron-phonon scattering which causes the increase of plasmonic damping constant with increase of the temperature leading to the weakening of the plasmonic enhancement. Second one is the thermal expansion of the gold NPs. The thermal expansion increases the NP size leading to decrease of the plasmonic damping caused by surface scattering of electrons and to corresponding strengthening of plasmonic enhancement. The results of theoretical calculations agree with the results of the experimental observations proving the model used. The calculations showed that the electron-phonon scattering is prevailing mechanism in the temperature dependence of the factor of plasmonic enhancement of PL from R6G on Au NPs as compared to effects related to the thermal expansion of Au NPs.

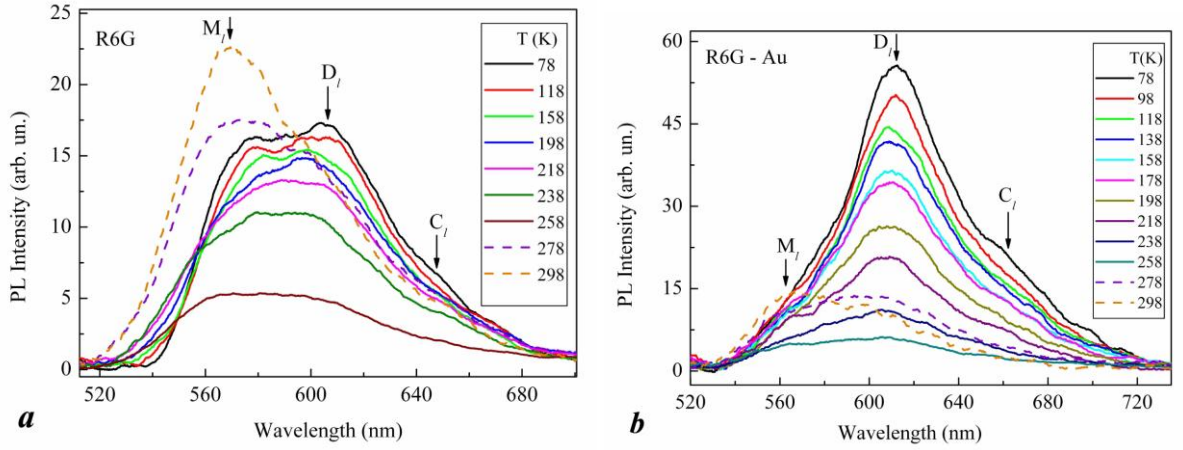

Figure 1. Evolution of PL spectrum of R6G/shellac thin film (a) and one of R6G/shellac thin film deposited on Au NPs array with monotonous increase of temperature from 78 to 298 K.

yes@univ.kiev.ua

An Direct Comparison of Plasmonic and Interband Hot Carrier Generation

Bob Zheng[1,4], Hangqi Zhao[1,4], Alejandro Manjavacas[2,4], Michael McClain[3,4], Peter Nordlander[2,4], Naomi Halas[1,2,3,4]
[1]*ECE, Rice University, Houston, Texas, USA*
[2]*Physics and Astronomy, Rice University, Houston, USA*
[3]*Chemistry, Rice University, Houston, USA*
[4]*Laboratory for Nanophotonics, Rice University, Houston, USA*

Hot carrier generation in metallic nanostructures offers a potential route to circumventing thermodynamic efficiencies of traditional light-harvesting devices and structures. However, previous experimental realizations of hot electron devices have shown low photo-conversion efficiencies. Several theoretical works have sought to understand the fundamental processes behind hot carrier generation and explore routes toward increasing the carrier generation efficiency. In this work, we discriminate between hot carrier generation from interband transitions and surface plasmons by comparing photocurrent generation in Schottky and ohmic devices. We show that plasmonic hot carrier generation results in high energy hot carriers while hot carriers from interband transitions result in low energy carriers. We also show that plasmonic hot carrier generation depends on the field intensity enhancement and independent of interband absorption. This work definitively shows that plasmonic hot carrier generation is not explained by heating and shows that injection of hot carriers over an energy barrier explicitly requires surface plasmon decay. Our results also show a surprising deviation from Fowler theory, which indicates that surface plasmons preferentially excite electronic states near the Fermi level. This work paves the way for more efficient hot electron devices and could lead to the development of novel optoelectronic devices.

byz1@rice.edu

Nanoparticle-Assisted Solar Alcohol Distillation

Oara Neumann[1,6], Albert Neumann[3], Edgar Silva[4], Ciceron Ayala-Orozc[5,6], Shu Tian[5,6], Peter Nordlander[2,6], Naomi Halas[1,2,5,6]

[1]*Department of Electrical and Computer Engineering, Rice University, Houston, Texas, USA*

[2]*Department of Physics and Astronomy, Rice University, Houston, Texas, USA*

[3]*Department of Civil and Environmental Engineering, Rice UIniversity, Houston, Texas, USA*

[4]*Department of Mechanical Engineering, Rice University, Houston, Texas, USA*

[5]*Department of Chemistry, Rice University, Houston, Texas, USA*

[6]*Laboratory for Nanophotonics, Rice Quantum Institute, Houston, Texas, USA*

Solar-based distillation methods have the potential to significantly reduce the current energy-intensive distillation processes. This method is based on the use of metallic light-harvesting nanoparticles that capture solar energy for direct liquid-vapor conversion, an inherently non-equilibrium vaporization process, eliminating the energy requirement of heating the entire fluid volume. To further investigate the effect of the metallic nanoparticles on the distillation process, two azeotropic systems, with different hydrogen bonding network strength, ethanol-water and 1-propanol-water mixtures were selected. In the case of nanoshell-ethanol-water mixtures, the mole fraction of ethanol obtained in the laser induced distillation process was higher than that obtained by thermal flash distillation process. Additionally, in a controlled N_2 environment that avoids vapor water contamination, the ethanol-water azeotrope was overcome. In contrast, in the case of nanoshell-1-propanol-water mixtures the mole fraction resulted from laser induced distillation process was found to be equivalent with the thermal distillation process without significant shift in the azeotrope. Additionally, when the nanoshells-1-propanol-water mixtures with 0.49-0.9 1-propanol mole fraction were illuminated from the top, a phase separation was observed. The top solution that contains the flocculated nanoparticles is richer in 1-propanol content compared with the bottom solution. However, the laser induced nanoshells flocculation is a reversible process and the nanoshells maybe redispersed by shaking the container.

on4166@rice.edu

Plasmonic and Silicon Nanoparticle Coatings for Thin-Film Photovoltaic Applications

Mihail Petrov[1,2], Ksenia V. Baryshnikova[1], Viktoriia E. Babicheva[1], Pavel A. Belov[1]

[1]*IRC Nanophotonics and Metamaterials, University of ITMO, Saint-Petersburg, Russia*

[2]*Condensed Matter Physics, Saint-Petersburg Academic University RAS, Saint-Petersburg, Russia*

Thin-film solar cells is rapidly growing sector of photovoltaics industry, but the wide range of possible applications is limited by their low efficiency of light absorption in the thin active layer. Plasmonic light trapping coatings were suggested as promising candidate to overcome this problem. Later it has been proposed to implement dielectric and semiconductor nanoparticles with high refractive index for light trapping. In this work we present a comparative analysis of plasmonic and semiconductor light trapping coatings based on periodic arrays of spherical silver, gold, and silicon nanoparticles. We have restricted the parameters of the structure to allow only dipole nanoparticle resonances in the optical range. Our calculations show that silver and silicon coatings demonstrate much higher absorption enhancement comparing to gold coatings. Although, integral enhancement with silicon coating is comparable to silver one, silicon coatings provide an advantage in terms of practical applications, as they are not subjected to aging in comparison to silver coatings. We also dem onstrate that silver and silicon coatings completely suppress reflection at particular frequency because of interaction of electrical and magnetic modes inside the particle, which results in peak-absorbance enhancement in the region between the resonances. This effect is associated with Huygens-like properties of silicon nanoparticles. Moreover, silicon based coatings have narrow banded absorption enhancement in between the magnetic and electric resonances with spectral position strongly dependent on nanoparticle radius. The obtained calculation results show potential applicability of silicon nanocoatings for thin-film photovolatics.

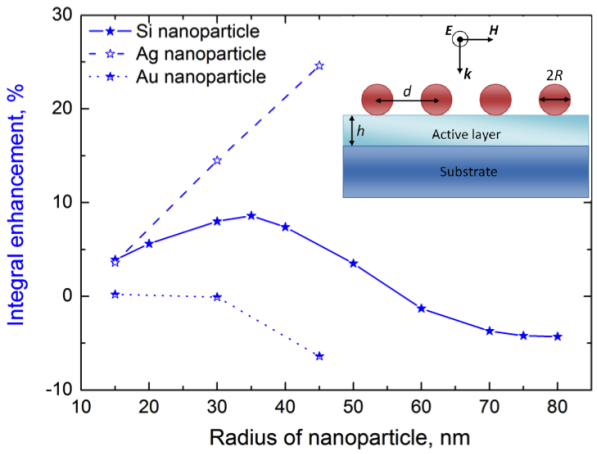

Figure: Integral enhancement for different type of coatings. Inset: 2D periodic array of spherical nanoparticles with radius *R* on the top of a-Si:H active layer. The active layer (light blue) is on top of the bulk substrate (dark blue). The period of the structure is and the thickness of the active layer is *h*. The direction of incidence is also shown by the direction of wave vector *k*.

trisha.petrov@gmail.com

Light Trapping in Thin Silicon Substrate: Exciting Insights from Aluminum versus Gold Nanoplasmonic Simulations

Sruthi Venkataramana Babu, Apoorva Agarwal, . Shahela, Anirudh Ramesh, Manav Shah, Devesh Jain, Harikrishnan Vasudevan, Kannan Ramaswamy
Physics, Birla Institute of Technology and Science, Hyderabad, Telangana, India

The efficiency of photocurrent generation in a thin film solar cell is low due to incomplete absorption of incident solar radiation. Light trapping techniques such as the coupling of surface plasmons with the incident electromagnetic radiation can lead to enhanced absorption and photocurrent generation.[1] Apart from the conventional plasmonic metals like gold (Au) and silver, aluminum (Al) has also been reported to exhibit exciting plasmonic properties.[2]

We carried out Finite DifferenceTtime Domain (FDTD) simulations to compare the intensity of the scattered electric field, electron-hole pair generation rate (G_{opt}) and the photocurrent generation inside a thin silicon (Si) substrate patterned on the surface with Au and Al nanospheres. Even though Au has better plasmonic properties in the wavelength region of interest (AM1.5), our simulations indicate that the substrate patterned with Al nanospheres yield short circuit current density (J_{sc}) (112.57 A/m^{2-}) higher than that obtained with Au nanospheres (78.08 A/m^2).[3] Furthermore, the sensitivity of Al towards oxidation has been a major deterrent in its use as a plasmonic metal. Simulations indicate that even Al_2O_3 coated (6 nm) Al yields a higher value of J_{sc} (87.86 A/m^2).

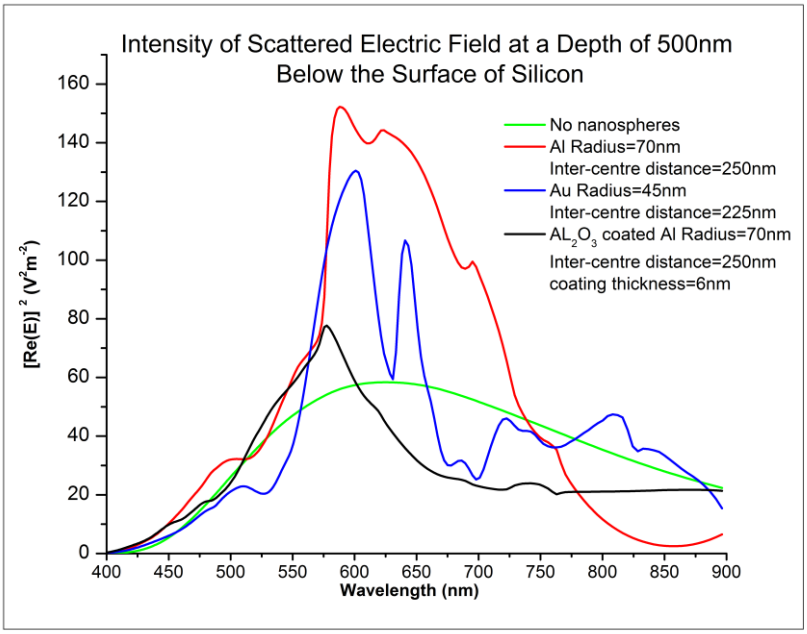

Figure 1 shows that the electric field intensities for Al and Au are comparable. However, they do not translate into higher values of G_{opt} and J_{sc} for Au (Fig.2). This could be attributed to -the dependence on the light source used to determine J_{sc}.

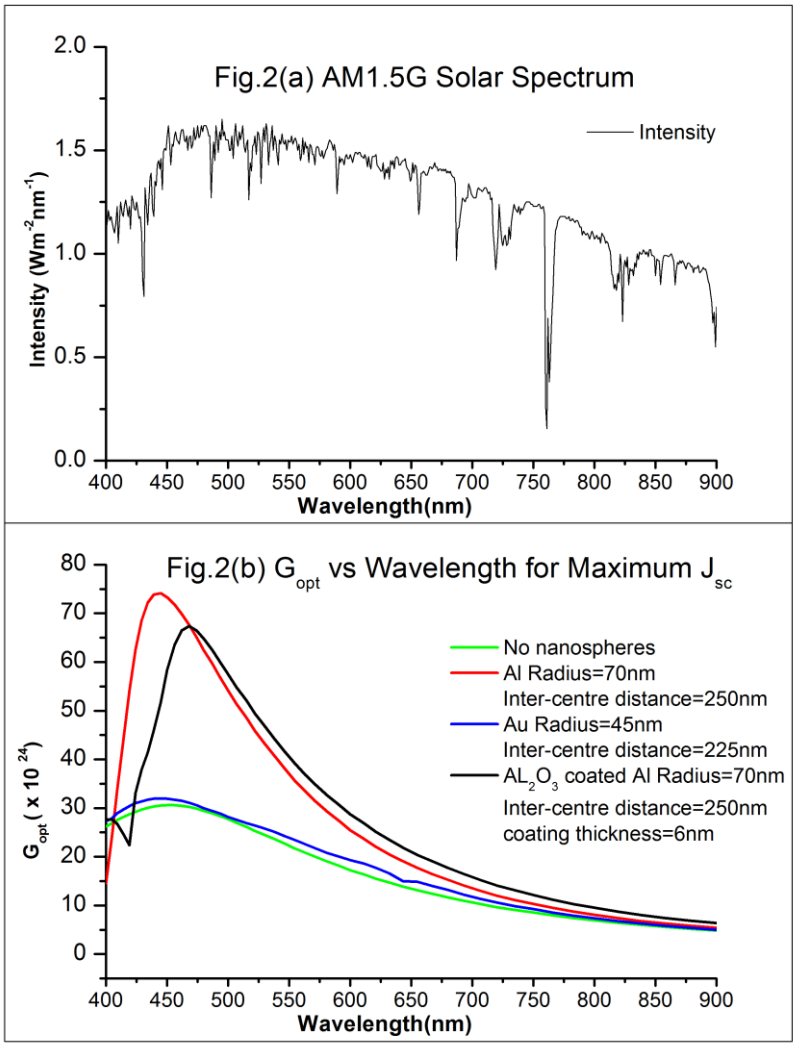

In summary, our simulations using Al nanospheres on thin Si substrate indicate the potential of Al to replace conventional plasmonic metals to enhance the photovoltaic efficiency of Si based thin-film solar cells.

[1]. Atwater, H. A; Polman, A. *Nature Materials*, 2010, **9**, 205-213

[2]. Knight *et al*. *ACS Nano*, 2014, **8**(1), 834-840

[3]. Stockman, M. I; *Optics Express*, 2011, 19(22), 22029-22106

sruthi.v1994@gmail.com

Compensating Plasmonic Losses with Infinite Energy Beams

Itai Epstein, Yuval Tsur, Ady Arie
Physical Electronics, Tel Aviv University, Tel Aviv, Israel

While surface-plasmons exhibit unique and attractive properties such as high-spatial confinement and enhancement of the optical field, they also suffer from inherent ohmic losses. The latter is probably the most pronounced fundamental challenge in the field of plasmonics and a true bottle-neck for many applications and industrial implementation. For this reason there has been an increased scientific interest in recent years, to find new ways to overcome this loss issue in plasmonic systems. These include the use of various gain media, lasing, novel hybrid wave-guiding with decreased losses, and more. Recently, it was suggested and demonstrated that free-space self-accelerating beams, i.e. – multiple-lobed, non-diffracting curved beams, can be used in order to compensate for absorption losses of the beam's main lobe by enhancing the energy of its side-lobes [1, 2]. It was suggested that this solution may enable to compensate for plasmonic losses as well.

In this work, we demonstrate both numerically and experimentally, the first realization of the above-mentioned concept with surface-plasmons waves. We further extend the concept beyond self-accelerating beams, into non-diffracting beams that propagate along straight trajectories which are more suitable for on-chip communication, waveguide coupling and nanotechnology applications. As an example, Fig.1 shows experimental measurements of (a) a regular self-accelerating plasmonic Airy beam, exhibiting decay of the main`s lobe intensity and (b) a loss-compensated Airy-beam, in which the intensity of the main lobe is preserved (Fig.1(b)).

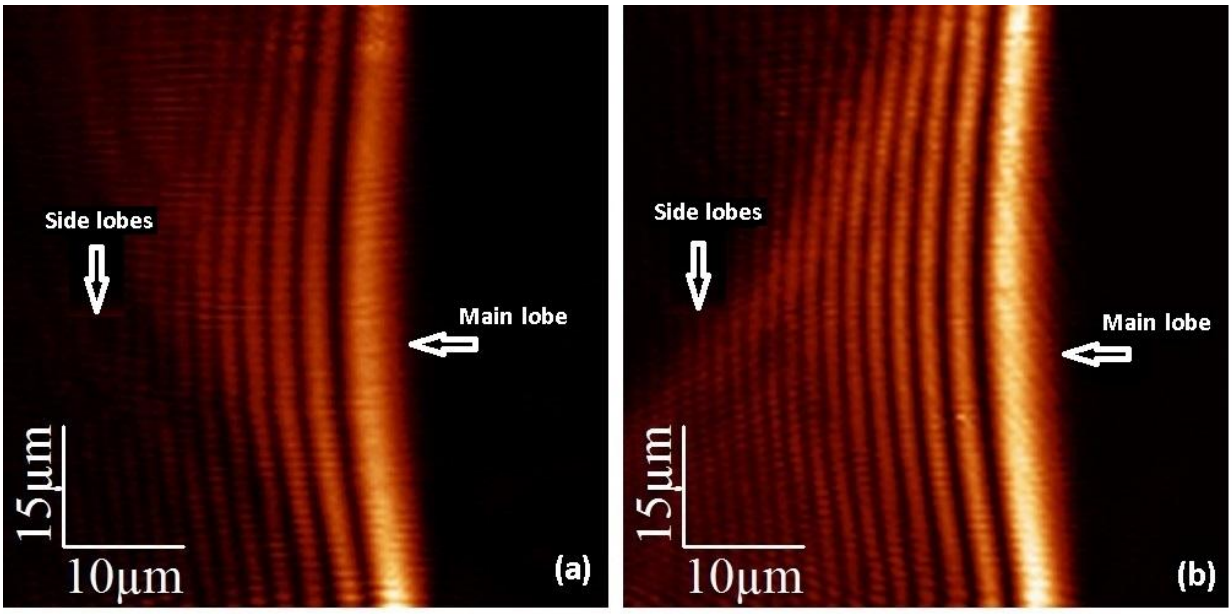

Fig.1: Experimental measurement of the intensity distribution of (a) a regular and (b) a loss-compensated plasmonic self-accelerating Airy beam.

By extending the propagation length of surface-plasmons, we believe that this demonstration will pave the way for new and exciting applications in plasmonics, such as on-chip communication technologies, particle micromanipulation, nonlinear plasmonics and more.

[1] Perciado et al, Opt. Lett 39, 4950 (2014)

[2] Schley et al, *Nat. Comm. 5*, 5189 (2014).

itayet@post.tau.ac.il

Surface Plasmon Laser based on Au Nanoparticles in a Solution for Visible and Near IR Region

Fedor Benimetsky[1], Tamara Basova[2], Roman Parkhomenko[2],
Aleksander Kuchyanov[1], Aleksander Plekhanov[1]
[1]*Physics of Laser laboratory, Institute of Automation and Electrometry of the Siberian Branch of the Russian Academy of Science, Novosibirsk, Russia*
[2]*Laboratory for Chemistry of Volatile Coordination and Metallorganic Compounds, Nikolaev Institute of Inorganic Chemistry of the Siberian Branch of the Russian Academy of Science, Novosibirsk, Russia*

Bergman and M. Stockman proposed spaser in 2003 [1]. Recently, the lasing action of gold nanospheres in a dye-filled, glasslike shell immersed in a solution has been demonstrated [2,3] including three-dimensional lasing spaser made of photonic crystal containing self-assembled gold nanoparticles in dye-doped shell [3].

The spaser is analogous to the conventional laser. A spaser consists of a metal nanoparticle (NP) as the resonator surrounded by a nanoshell of the gain medium. In contrast, the spaser as a nanoscopic quantum generator of localized surface plasmons is a promising candidate for a wide range of applications because it allows beating the diffraction limit and focusing electromagnetic energy to spots much smaller than a wavelength.

Despite the first successful demonstration of spasing, no experimental demonstration of the spaser effect in a solution has ever been observed. However, overcoming these experimental difficulties enables the opportunity to demonstrate their potential applications, for example, in biomedicine [4].

Here, we experimentally demonstrate spasing in a solution of hybrid Au nanoparticles for visible and near IR region. To produce spasers we have fabricated hybrid nanoparticles with a 10-nanometre gold core or nanorods with a different aspect ratio surrounded by a 20-40-nanometre-thick silica shell, embedded with dye molecules (fluorescein or DCM). Here, progress in the study of spasers will be presented.

This work was supported by RFBR Grants 15-03-03833, 15-02-02333, RAS#19.

(1) Bergman, D.; Stockman, M. *Rev. Lett*. **2003**, *90*, 027402.

(2) Noginov, M.; Zhu, G.; Belgrave, A; Bakker, R.; Shalaev, V; Narimanov, E; Stout, S.; Herz, E.; Suteewong, T.; Wiesner, U. *Nature* **2009**, *460*, 1110-1113.

(3) Kuchyanov A.S, Igumenov I.K., Kuchumov B.M., Parkhomenko R.G., Chang-Won Lee, Young-Geun Roh, Heejeong Jeong, Stockman M.I., and Plekhanov A.I. External-cavity spasers. Proceedings of the Eights International Conference on Material Technologies and Modeling MMT-2014, July 28 -August 01 2014, Ariel, Israel, p.2-81-88.

(4) Galanzh E.I., Weingold R., Nedosekin D.A., Sarimollaoglu M, Kuchyanov A.S., Parkhomenko R.G., Plekhanov A.I., Stockman V.I., Zharov V.P. Spaser as Novel Versatile Biomedical Tool. **2015,** arXiv 1501.00342

benimetsky@gmail.com

Heating and Cooling in Electrically Pumped Plasmonic Structures

Andrey Vyshnevyy, Dmitry Fedyanin
Laboratory of Nanooptics and Plasmonics,
Moscow Institute of Physics and Technology, Dolgoprudnyy, Russia

Metal-semiconductor plasmonic waveguides provide strong mode confinement and are considered to be prospective candidates for on-chip interconnects. However, very short propagation lengths prevent their practical utilization. This limitation can be overcome by compensating for ohmic losses in the metal by optical gain in the adjacent semiconductor. For chip scale integration, pumping and plasmonic waveguides must be integrated on a single chip, which can be achieved with electron and hole injection into the active semiconductor region of the active plasmonic structure. However, inspite of the high efficiency of electrical pumping, the current density approaches 10kA/cm^2 in the regime of full loss compensation, which corresponds to a power consumption per unit waveguide length per unit waveguide width of about 5 kW/cm^2. It is not difficult to see that this value greatly exceeds the average heat generation of the microprocessor chip (~100W/cm^2). This can cause heating of the active region and reduce the device performance or even destroy it.

In this work, we study heating and cooling of the electrically pumped active plasmonic waveguide (see fig. 1a). Device is placed under 500 nm layer of Al followed by the 150μm of solder and 1-mm-thick Al bulk. Solving self-consistently the electron and hole transport equations together with the thermal conductivity equation, we find the temperature distribution in the active InAs region. In the regime of full loss compensation, at an average waveguides spatial density of 17 mm^{-1}, electrical pumping does not heat the device: the temperature nearby the Au/InAs contact is only 2.8 K above the ambient temperature (fig. 1b). As the SPP power increases to 10 mW, the maximum temperature increases up to 54 K above the ambient temperature due to the substantial increase in the current density required for full loss compensation. At a practical SPP power of 0.2-1mW, the waveguide heating is very small and can be neglected.

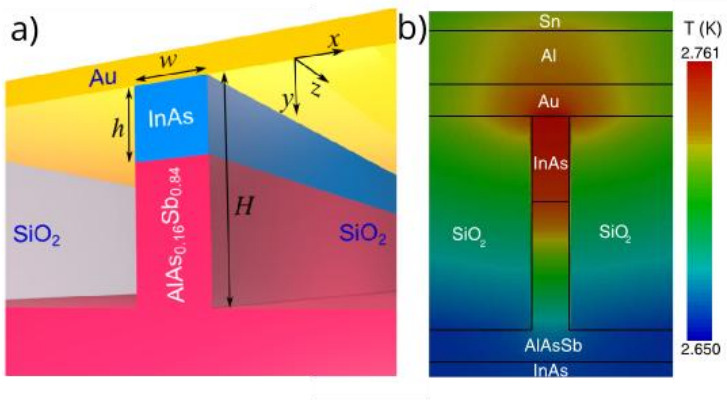

Fig. 1. (a) Schematic of the active plasmonic waveguide. (b) Temperature distribution (with respect to the ambient temperature) in the waveguide cross-section at a low SPP power.

andervish@gmail.com

An Active-Tuned Plasmonic Modulator by Voltage

Hailong Wang, Shuping Xu, Haibo Li, Cucui Fu, **Xu Weiqing**
State Key Laboratory of Supramolecular Structure and Materials, Institute of Theoretical Chemistry, Jilin University, Changchun, China

Plasmonic modulators controlled by electrical signal have attracted many researchers due to their advantages of being the bridge between electrics and optics, and the compatibility with existing integrated electronic circuits.[1] In this work, we utilized liquid crystal (LC) molecules as a medium to control the extraordinary optical transmission (EOT) of light through a grating structure by applying electrical signals on LC. And the potential application as a wavelength modulation element in a plasmonic laser device was investigated.

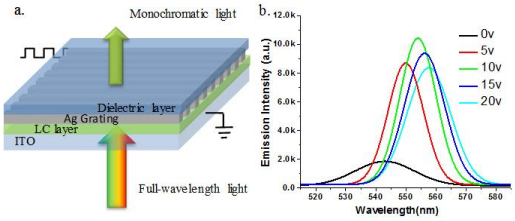

Figure 1 (a) The configuration of the LC-tuned plasmonic modulator based on the EOT mechanism. (b) The emission spectra of SPPs with different voltages applied on LC.

Fig. 1 (a) shows the configuration of the plasmonic mudulator. The key element in the modulator is an Ag double-side gratings, which was obtained by vacuum evaporation deposition of Ag (thickness= 70 nm) above a grating template. Between Ag gratings and ITO, a LC molecule layer (thickness=50 μm) was fabricated by the siphonic effect. When voltage signal (0-20 V) was applied on the Ag gratings and ITO, the rafractive index of the LC layer changed along (from 1.55 to 1.71). On the other side of the Ag grating, we spin-coated a dielectric layer as a refractive index maching layer (n=~1.7). When an normal incident light irradiated on the Ag/LC interface, the surface plasmon polaritons (SPPs) will be excited by a mono-wavelength lightwave with a grating mode, which is sensitive to the refractive index of the liquid crystal layer that can be active-tuned by applied voltage. On the other side of the Ag grating, the same mono-wavelength lightwave will shine out due to the EOT effect. Therefore, a monochromatic beam will radiate to far field. From Fig. 1 (b) that voltage-tuned SPPs emission spectra, we can find that the central wavelength of the SPPs emission shows a red shift with the voltage applied on the LC increasing. This result proves that this plasmonic modulator can be used as a wavelength modulation element when composed with plasmonic laser devices.

Acknowledgements: This work was supported by the National Instrumentation Program (NIP) of MSTC (2011YQ03012408) and NNSFC (21373096).

References:

[1] Lee, H. W., et.al, Nano letters, 14(11),6463-6468 (2014).

xuwq@jlu.edu.cn

Excitation of Radially Polarized Conical Surface Plasmon Polariton

Norik Janunts[1], Bayarjargal Tugchin[1], Angela Klein[1], Michael Steinert[1], Dmitry Sivun[2], Miguel Sison[3], Ernst-Bernhard Kley[1], Andreas Tünnermann[1], Thomas Pertsch[1]

[1]*Institute of Applied Physics, Friedrich-Schiller-Universität Jena, Jena, Germany*
[2]*Institute of Applied Physics, Johannes Kepler University Linz, Linz, Austria*
[3]*Laboratoire d'Optique Biomedicale, Ecole Polytechnique Federale de Lausanne, Lausanne, Switzerland*

We demonstrated experimentally the excitation of the radially polarized surface plasmon polariton (SPP) in a tapered and fully gold coated M-profile fiber (Fig. 1) which works as a Kretschmann configuration in conical geometry. The excitation process is based on the resonant coupling of the radially polarized fiber mode (Fig. 2) to the radially polarized SPP on the conical gold layer covering the tapered fiber. Due to the coupling the energy transfers from the fiber mode to the SPP mode (Fig. 3).

The SPP gets localized at the nano-scale apex of the tip producing a strong longitudinal field oscillating along the tip axis, and as a result emits to the side (Fig. 4). To probe the near-field characteristics at the tip apex, we placed the tip perpendicularly on a plane gold surface and studied the planar SPP generated on the plane gold surface by the tip (Fig.5). The SPP was shown to be radially polarized and radially symmetric.

We also demonstrated the reverse process when the induced longitudinal field at the tip apex serves as a source of conical radially polarized SPP originating from the tip apex.

norik.janunts@uni-jena.de

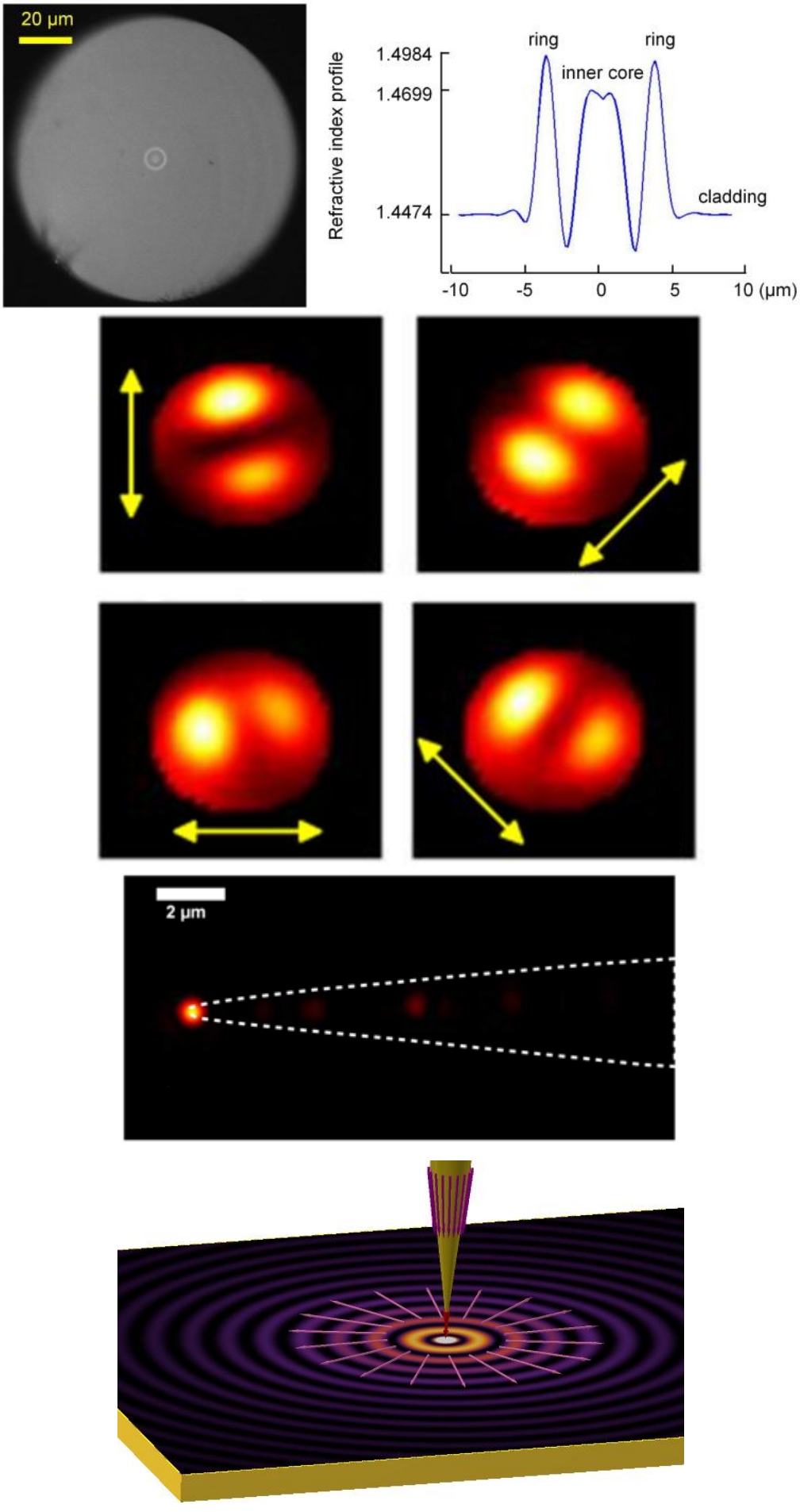
20 μm
Refractive index profile
1.4984
1.4699
1.4474
ring
ring
inner core
cladding
-10
-5
0
5
10 (μm)
2 μm

Plasmonic Resonances in Carbon Microfibres for Engineerable Terahertz Absorption

Irina Khromova[1,2,3], Oleg Mitrofanov[1], Miguel Navarro-Cia[1], Inigo Liberal[3], Igal Brener[4], John Reno[4], Leonid Melnikov[5], Andrey Ponomarev[6]

[1]*Department of Electronic and Electrical Engineering, University College London, London, UK*

[2]*The International Research Centre for Nanophotonics and Metamaterials, ITMO University, St. Petersburg, Russia*

[3]*Department of Electrical and Electronic Engineering, Public University of Navarra, Pamplona, Spain*

[4]*Center for Integrated Technologies, Sandia National Laboratory, Albuquerque, USA*

[5]*Chair of Instrumentation Engineering, Saratov State Technical University, Saratov, Russia*

[6]*-, Scientific Technical Centre of Applied Nanotechnologies, St. Petersburg, Russia*

We performed near-field time-domain spectroscopy on individual milled carbon microfibres (CMFs) to verify the presence of strong plasmonic resonances at terahertz frequencies. These plasma-chemically treated microfibres are 7 μm in diametre and their lengths vary from 10 μm to 150 μm. Fig.1 shows: (a) a SEM image of the CMFs, and (b) a space-time THz near-field map and (c) an image of a of a 133μm-long CMF. The terahertz conductivity of CMFs was extracted from the shift between the frequencies of an individual CMF absorption peak and the resonance frequency of the corresponding perfectly conducting dipole. Its value lies very close to the condition of maximum absorption to scattering relation.

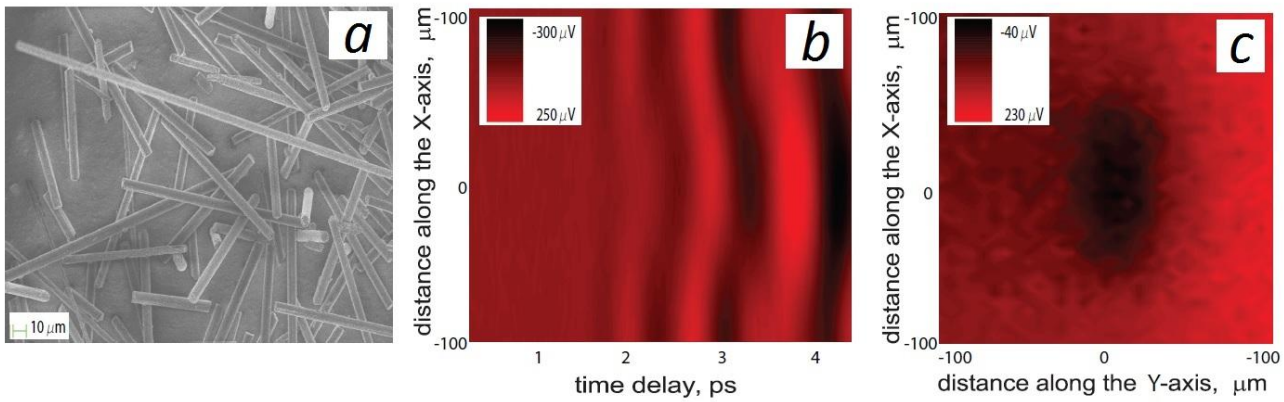

We used semi-analytical models to predict the usability of CMFs for efficient terahertz absorbers with engineerable response. Combining the effective medium approximation with a simple dipole antenna model, we numerically obtained scattering and absorption characteristics of composites containing CMFs with given lengths distributions.

We experimentally studied the terahertz response of thin pellets of high density polyethylene (HDPE) with arbitrarily oriented and differently sized CMF inclusions. These samples demonstrated a clearly resonant behaviour: broad absorption peaks at around 1.5 THz indicate the presence of size effects distributed over lengths of CMFs in each sample.

With artificialy created distribution of lengths, CMF-based composites may be designed according to desirable absorption profiles. This simlpe and inexpensive technique may, in particular, be used to achieve flat absorption at terahertz frequencies.

aerialcrystal@gmail.com

Mapping and Interpreting the Near Fields of Plasmonic Antennas

Tomáš Neuman[1,2,4], Pablo Alonso-González[3], Aitzol Garcia-Etxarri[1,2], Pablo Albella[1,2], Rainer Hillenbrand[3], Javier Aizpurua[1,2]

[1]*Material Physics Center, Spanish National Research Council and University of the Basque Country, San Sebastián, Spain*

[2]*Donostia International Physics Center, DIPC, San Sebastián, Spain*

[3]*Nanophotonics Laboratory, CIC nanoGUNE, San Sebastián, Spain*

[4]*Central European Institute of Technology, Brno University of Technology, Brno, Czech Republic*

Plasmonic antennas concentrate and enhance electromagnetic fields into regions below diffraction limit. Advanced theoretical and experimental techniques are necessary to fully characterize the antenna near fields [1], as in scattering-type Scanning Near-field Optical Microscopy (s-SNOM), accessing both the near-field amplitude and phase. The cross-polarized detection scheme utilized in the s-SNOM measurements enables to distinguish the signals recorded in S- and P-polarizations [2]. Here we review and modify the common assignment of the S- and P-resolved signals to the in-plane and out-of-plane components of the local near field around the antenna, respectively.

We interpret the s-SNOM signal obtained with use of weakly scattering tips as a scalar product of the real antenna electric near field and a virtual electric field which would be induced in the antenna by a source placed at the position of the detector with the same polarization as the detected light. We demonstrate theoretically and experimentally that the s-SNOM near-field signal measured on single and dimer plasmonic antennas can be understood as a result of a mixing of the antenna electric near-field components rather than measurement of the in-plane or out-of -plane electric fields.

The novel signal interpretation of s-SNOM images verifies a quadratic dependence of the signal amplitude on the antenna near-field enhancement resembling the enhancement mechanism in field enhanced spectroscopies [3]. S-SNOM is an ideal tool for local characterization of the antenna near-fields, but as shown here, an appropriate interpretation of the signals is required for a correct understanding of the images.

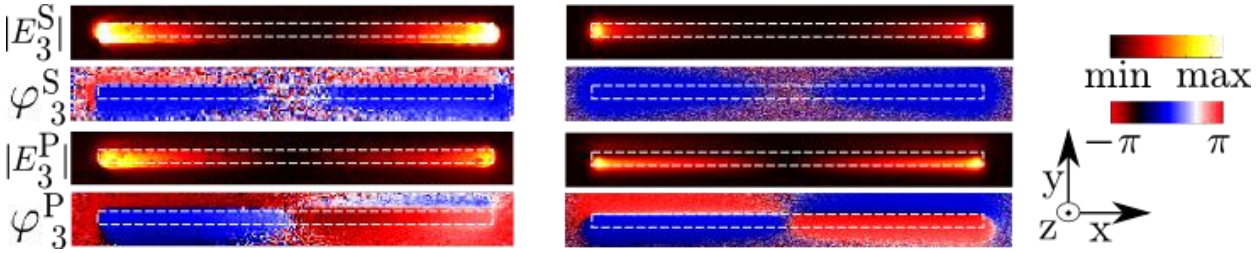

Fig. 1: Experimental (left) and theoretical (right) near-field maps of a linear dipole antenna. The antenna length is 3.2 μm and the probing wavelength is λ=11.06 μm.

[1] P. Alonso-González *et al.*, *Nano Lett.* **11**, 3922 (2011).

[2] M. Schnell *et al.*, *Nano Lett.* **10**, 3524 (2010).

[3] P. Alonso-González *et al.*, *Nature Comm.* **3**, 684 (2012).

[4] T. Neuman *et al.*, (submitted)

tomas_neuman001@ehu.es

Robust Point-to-Point Near-Field Lensing by a Double-Negative Single-Interface

Gilad Rosenblatt, Meir Orenstein
Department of Electrical Engineering, Technion-Israel Institute of Technology, Haifa, Israel

Typical working near-field imaging schemes employ a scanning apparatus, e.g. a sensing tip whose finite size and scattering efficiency determine resolution. Using a double-negative (DNG) medium slab as a non-scanning perfect-resolution imaging device, while a conceptually pioneering idea, has thus far proved inapplicable due to very high sensitivity to intrinsic DNG media loss and the ultra-narrow band of the effect.

Here we propose a lensing configuration which can in principle overcome these difficulties, with potential for actual application. It is realized by a simple single-interface between a regular dielectric (DPS) containing the source (imaging object) and a DNG metamaterial containing an ideal detection element (drain) – where a perfect image is formed (Fig. 1a). The unexpected robustness of this configuration is arrived at by modal, scattering (reflection and transmission), and excitation (Green) studies. Perfect point-to-point lensing is maintained even under realistic material loss and/or excitation frequency offsets, mainly since the optical transfer function (Fig. 1b-d red) remains a spatial all-pass filter (rather than a low-pass as with the DNG slab lens, green).

The modal lensing mechanism relies solely on excitations of an 'improper' (double-diverging) Brewster mode in between the source and image planes, whose flat dispersion (Fig. 1e) allows for its excitation and subsequent reflectionless transmission at any spatial frequency.

Practical limitations to resolution are concerned with two controllable factors: the quality and density (pixel-size) of detection elements, and the exposure time necessary for a desired resolving power (perfect focusing only forms at the stationary limit).

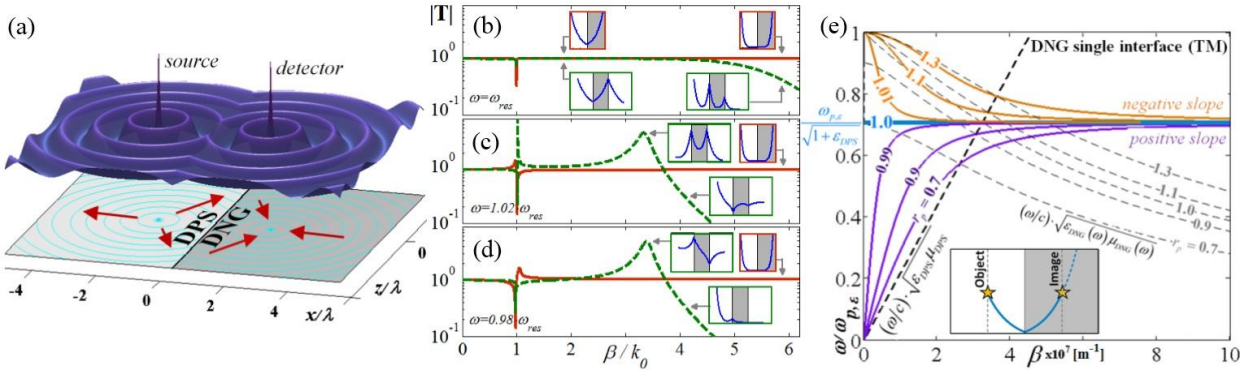

Fig. 1. (a) Stationary field solution for a point-source excitation perfectly „copied" by a lossless DNG-DPS single-interface onto a point-drain (power direction, red). (b-d) Amplitude transmission vs. propagation constant β for lossy single-interface (red) and slab (green) lenses at several frequencies (inset: field profile at indicated points). (e) Brewster mode (inset) dispersion curve at matched ($\mu_{DPS}/\varepsilon_{DPS}=\mu_{DNG}/\varepsilon_{DNG}$, blue) and mismatched conditions ($r_p=\omega_{p,\mu}/\omega_{p,\varepsilon}$ values indicated). $\varepsilon,\mu_{DNG}=1-\omega^2_{p,\varepsilon,\mu}/\omega(\omega+i\cdot\omega_{\tau,\varepsilon,\mu})$, $\varepsilon,\mu_{DPS}=1$, $\omega_{p,\varepsilon}=1.37\cdot10^{16}$, $\omega_{res}=\omega_{p,\varepsilon}/(1+\varepsilon_{DPS})^{1/2}$.

tuna@tx.technion.ac.il